Geological Quarterly, 2024, 68, 38
DOI: http://dx.doi.org/10.7306/gq.1766

# Organic matter thermal maturity analysis and modeling in the Paleozoic-Mesozoic section of the Miechów Trough (southern Poland): implications for thermal evolution

Dariusz BOTOR[1, *]

[1] AGH University of Kraków, Faculty of Geology, Geophysics and Environmental Protection, Al. Mickiewicza 30, Kraków 30-059, Poland; ORCID: https://orcid.org/0000-0003-0157-4885

Botor D., 2024. Organic matter thermal maturity analysis and modeling in the Paleozoic-Mesozoic section of the Miechów Trough (southern Poland): implications for thermal evolution. Geological Quarterly, 68, 36; https://doi.org/10.7306/gq.1766

Vitrinite reflectance analyses and 1-D thermal maturity modeling of the Paleozoic-Mesozoic section of the Miechów Trough have allowed interpretation of the thermal history that influenced hydrocarbon generation. The thermal maturity of organic matter dispersed in the Lower Paleozoic to Mesozoic sedimentary successions is in the range of 0.49 to 3.06% of mean random vitrinite reflectance. The estimated maximum palaeotemperatures of the rocks analyzed are in the range from ~70 to ~290°C. The Variscan thermal regime was different to the Mesozoic one. At least two fluid flow events might be identified. The maximum palaeotemperature (~120–290°C) in the Silurian to Lower Carboniferous sedimentary succession was achieved in the late Carboniferous to early Permian. The Late Variscan tectonic activity may have been triggered by increased heat flow that was, at least partly, connected with fluid circulation. The maximum palaeotemperature (~70–150°C) of the Zechstein to Jurassic sedimentary succession was achieved during the Mid-Late Jurassic. This was likely caused by a hot fluid flow event. The hydrocarbon potential of Paleozoic source rocks was exhausted before the Upper Jurassic and Cenomanian reservoir rocks and traps were formed. Consequently, the majority of hydrocarbons generated during the pre-Late Jurassic stages were lost.

Key words: vitrinite reflectance, thermal maturity modeling, Polish Basin, Carpathians Foredeep, petroleum origin, hydrocarbon generation.

## INTRODUCTION

A report on the latest balance of mineral resources deposits in Poland, published by the Polish Geological Survey, estimates reserves totaling ~142 BCM (5 TCF) of natural gas in 306 fields, and ~22 MTOE (157 MMBOE) of crude oil in 87 fields (cf. Wójcik et al., 2022). One of the important areas of oil and gas deposits in Poland is the Carpathian Foredeep and its Paleozoic-Mesozoic substrate (Karnkowski, 2007). The Miechów Trough, sometimes called the Nida Trough or Nida Depression, is developed as the southern part of the Polish Basin. The Miechów Trough in its southern part is overlain by Miocene strata of the Carpathians Foredeep, where thermogenic oil and gas accumulations occur mainly in Upper Jurassic carbonates and Cenomanian sandstones (e.g., Brzezowiec, Grobla-Pławowice, and Łąkta fields) in the Mesozoic basement (e.g., Gliniak et al., 2005; Górka et al., 2007; Słonka and Krzywiec, 2020). These oil and gas fields were likely charged by Paleozoic source rocks (e.g., Więcław et al., 2011; Kotarba et al., 2017) or by the Menilite Beds of the Outer Carpathians (Ten Haven et al., 1993; Curtis et al., 2004; Lewan et al., 2006; Nemčok and Henk, 2006; Botor, 2021). There are also gas fields in the autochthonous Miocene strata of the Carpathian Foredeep which contain almost exclusively bacterial gases (e.g., see recent summary in Kotarba et al., 2017 and further references). However, no petroleum deposits are known in the area north of the Miocene extent, despite many oil shows (Fig. 1; e.g., Jurkiewicz, 1975; Górka et al., 2007). The absence of a Miocene seal (Fig. 1) seems to be an important factor that drastically reduces prospects in this area (Papiernik et al., 2007).

Vitrinite reflectance (VR) is commonly applied as a palaeotemperature indicator in sedimentary rocks and it serves as a calibration tool in numerical modeling of the thermal histories of sedimentary basins (e.g., Waples et al., 1992a, b; Hantschel and Kauerauf, 2009; Hartkopf-Fröder et al., 2015; Zielińska, 2017; Waliczek et al., 2019, 2021; Kalinowski and Gurba, 2020; Zielińska et al., 2023). Since the early publication of Waples (1980) the numerical simulation of subsidence, burial, and the thermal histories of sedimentary basins became a widely used method in geology (Hantschel and Kauerauf, 2009 and references therein). It is applied in petroleum exploration, where processes such as hydrocarbon generation, migration and accumulation are studied (e.g., Waples et al., 1992a, b; Verweij et al., 2012; Botor et al., 2019). Such modeling techniques are also used to solve basic geological questions such as the controls on palaeothermal regimes, tectonic inversion, and orogenic processes (e.g., Resak et al., 2008; Narkiewicz et al., 2010; Suchý et al., 2019; Łuszczak et al., 2020; Zielińska et al., 2023). This study reconstructs the regional palaeotemperature pattern and burial evolution of the Miechów

* E-mail: botor@agh.edu.pl

Received: July 5, 2024; accepted: October 1, 2024; first published online: November 29, 2024

Trough by means of VR data. It enables recognition of particularly important and basic elements of the petroleum system such as temperature and pressure and its influence on the thermal maturity of organic matter and hydrocarbon (HC) generation. Combined VR analysis and thermal maturity modeling was applied to establish the burial and thermal history of the study area.

## GEOLOGICAL SETTING

The study area is located within the central part of the Miechów Trough (Figs. 1 and 2). To the SW the Miechów Trough passes gradually into the Silesian-Kraków Homocline, and to the NE into the Holy Cross Mountains (HCM) being a segment of the Mid-Polish Anticlinorium. The Miechów Trough forms the south-eastern segment of the Szczecin–Miechów Synclinorium (Żelaźniewicz et al., 2011), formation of which was completed during the Late Cretaceous–Paleogene tectonic inversion of the Permian-Mesozoic Polish Basin (e.g., Dadlez et al., 1995; Krzywiec, 2002; Resak et al., 2008; Krzywiec et al., 2018). The Permian–Mesozoic Polish Basin formed the easternmost part of a system of epicontinental basins in western and central Europe (Scheck-Wenderoth et al., 2008). Its most subsiding axial part – the Mid-Polish Trough – developed along the NW- to SE-trending Teisseyre-Tornquist Zone (Mazur et al., 2015). Tectonic inversion of the Polish Basin was associated with uplift and exhumation of the axial part of the basin, which was transformed into a regional anticlinal structure – the Mid-Polish Swell (e.g., Żelaźniewicz et al., 2011). Due to inversion-related development of the Mid-Polish Swell, two regional units were formed along both its flanks, including the south-western Szczecin–Miechów Synclinorium (e.g., Dadlez et al., 2000; Żelaźniewicz et al., 2011). The Permian-Mesozoic succession in the study area consists of Zechstein evaporite deposits, Triassic clastic rocks, carbonates and anhydrites, and Jurassic siliciclastic and carbonate rocks, Albian-Cenomanian sandstones and Turonian to Lower Maastrichtian marls, chalks and limestones (Jurkiewicz, 1975; Moryc, 2006b, 2014; Jurkowska, 2016). The southeastern part of Miechów Trough is overlain by the Miocene strata of the Carpathian Foredeep (e.g., Oszczypko et al., 2006).

The basement of the Permian-Mesozoic Miechów Trough is built of upper Proterozoic–Carboniferous rocks which are a part of the Małopolska Block (Buła et al., 1997, 2015), which extends between the Upper Silesian and Łysogóry blocks (Figs. 1 and 2). The pre-Devonian sedimentary cover has been intensely deformed and even, in the case of the Ediacaran rocks, partly metamorphosed (Buła et al., 2015). The final folding was probably associated with late Caledonian terrane accretion around the Silurian–Devonian boundary (Narkiewicz et al., 2020). The late Proterozoic–Paleozoic successions of the SW part of the Małopolska Block (basement of the Miechów Trough) include Proterozoic (Ediacaran), Ordovician (Tremadocian-Caradocian), Silurian (Llandovery-Ludlow), Devonian (Emsian-Famennian) and Carboniferous (Visean to Lower Namurian) rocks (Jurkiewicz, 1975; Moryc, 2006a, b, 2014; Buła et al., 2015). In the study area, Carboniferous strata were found in intervals of the Węgrzynów IG 1, Pągów IG 1 and Milianów IG 1 boreholes. In Węgrzynów IG 1 these are carbonate and clastic rocks of the Tournaisian and Visean, in Pągów IG 1 there are siltstones and sandstones of the Visean, and in Milianów IG 1 mudstone-sandstone strata of the Visean and Lower Namurian were penetrated (Jurkiewicz, 1974, 1975, 1976a, b, 1980, 1990). Malec (2015) showed, based on conodont stratigraphy, the presence of erosional stratigraphic gaps (Bretonnian phase) between the Devonian and the Carboniferous in the Pagów IG 1 and Węgrzynów IG 1 profiles.

The extensional regime prevailing in the Polish part of the southern Euramerica margin during most of the Devonian can be explained by slab-pull forces related to north-directed subduction of the Rheic oceanic plate (Narkiewicz, 2007, 2020). The extensional Devonian regime was interrupted by Bretonian tectonism in the beginning of the Carboniferous (Narkiewicz, 2007, 2020). Stratigraphic condensation and gaps spanning the uppermost Devonian and lower part of the Tournaisian have been noted in the Kielce area of the HCM (Szulczewski, 1995) and in the Upper Silesian region (Bełka, 1993). A sedimentary discontinuity at the base of the Mississippian, commonly labelled the Bretonian unconformity, has been postulated also in the southern part of the Małopolska Block (e.g., Żaba, 1999; Moryc, 2006a, b). Continuous sedimentation across the Devonian–Carboniferous boundary has been documented so far only locally in the HCM (Malec, 2015). However in some places in the HCM, continuity between Devonian and Carboniferous is present, for example in the Kowala quarry, and in the southern flank of the Gałęzice syncline (Rakociński et al., 2021).

The early Bashkirian (late Namurian A) was a time of non-deposition and erosion over the entire Variscan foreland area (e.g., Narkiewicz, 2020). K-Ar and Ar-Ar isotopic ages have corroborated the occurrence of minor mafic magmatism (lamprophyres and diabases) in the HCM (Migaszewski, 2002; Nawrocki et al., 2013). According to Lamarche et al. (2003a) the longitudinal discontinuities may represent inverted normal faults that developed due to Devonian extension. The Variscan structure of the MB south of the HCM displays faulted folds with an amplitude similar to those in the HCM, but with a considerably larger wavelength (Jurkiewicz, 1975; Papiernik et al., 2007; Buła et al., 2015). The results of palaeomagnetic studies impose rather wide constraints on the timing of the Late Paleozoic deformation in the HCM: from the Visean, when an early folding phase occurred, to the early Permian marking the termination of Variscan tectonism (Lamarche et al., 2003a; Szaniawski, 2008). Thus, the deformation might have started near the Visean–Serpukhovian boundary (~330 Ma) within a compressional regime which led to tectonic inversion and exhumation of the MB including the study area (see further discussion in Narkiewicz, 2020).

During the late Carboniferous to early Permian, intense granitoid magmatism developed within a wide belt along the Kraków-Lubliniec Fault Zone (KLFZ), which is a part of the major Hamburg–Kraków–Dobrogea transcontinental strike-slip tectonic zone (e.g., Żaba, 1999). The KLFZ delineates a boundary between the Upper Silesian Block and the Małopolska Block which is a thinned marginal part of Baltica (Buła et al., 1997; Żaba, 1999; Żelaźniewicz et al., 2016, and references therein). The KLFZ is also a part of the Trans-European Suture Zone (TESZ; Żelaźniewicz et al., 2016), one of the most important composite suture zones in Europe (Ziegler, 1986; Pharaoh, 1999). The fault crosscuts and offsets all Paleozoic and older rock units, including the Permian strata (Buła et al., 1997; Żaba, 1999). Igneous rocks that occur along the KLFZ are the products of bimodal magmatism, associated either with crustal thickening (Słaby et al., 2010) or with the dextral wrench regime and fault activity on the TESZ (Żelaźniewicz et al., 2016). Magmatism spanned a narrow time period between 304 and 293 Ma (Mikulski et al., 2019). Late Carboniferous to early Permian bimodal magmatism was likely related to the transition from a post-collisional to within-plate setting along the SW margin of the East-European Craton (Mikulski et al., 2019).

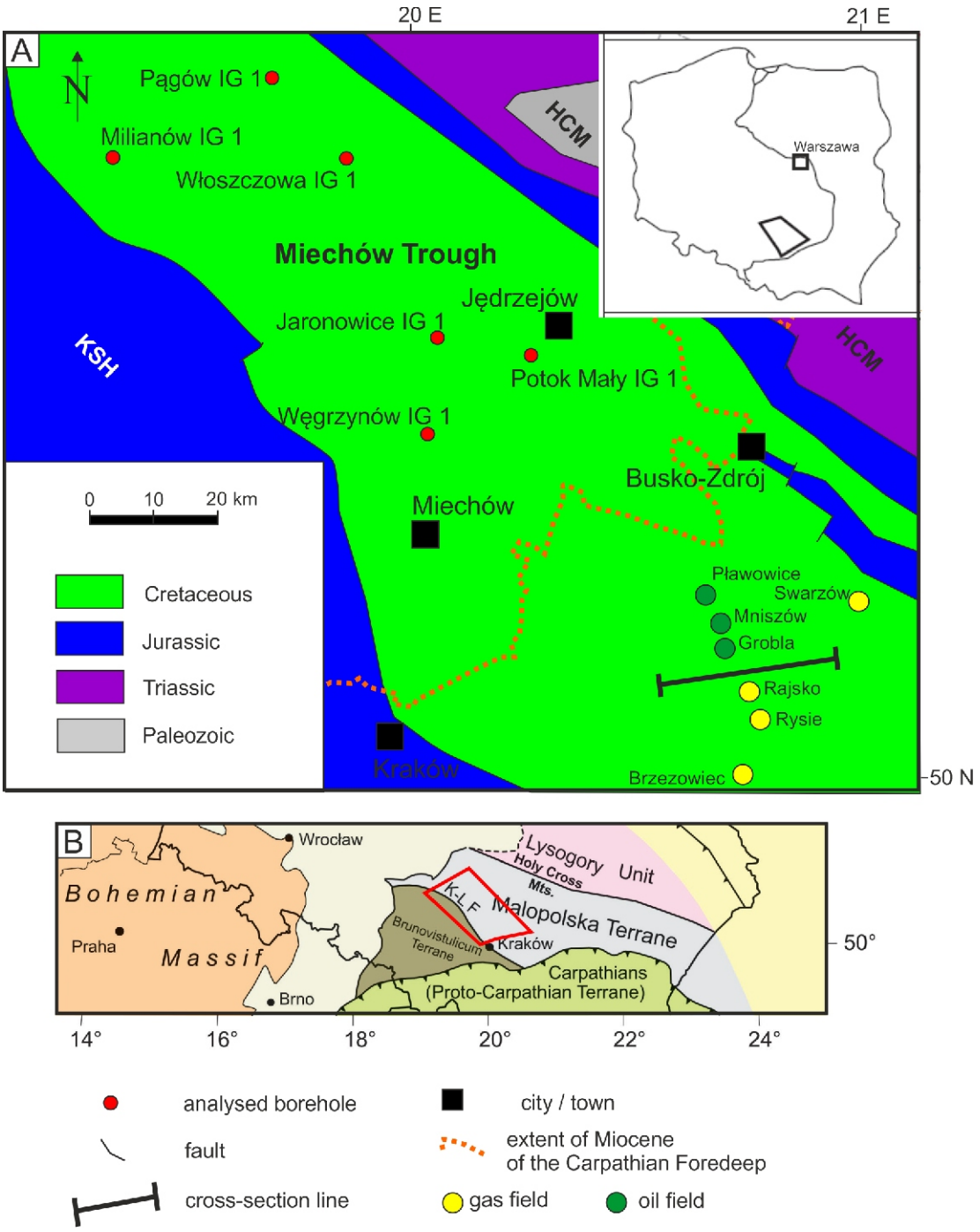


**Fig. 1A – location of the boreholes analysed on a simplified geological map of the study area without Cenozoic deposits (modified after Dadlez et al., 2000). Inset in the upper right corner shows the approximate position of the study area; B – sketch map of the main tectonic units of the sub-Permian basement of southern Poland and the surrounding area (modified after Mazur and Jarosiński, 2006; Nawrocki and Poprawa, 2006; Mazur et al., 2018)**

K-LF – Kraków-Lubliniec Fault

## PREVIOUS STUDIES OF THERMAL HISTORY

The thermal history of the entire south-western part of Małopolska Block is discussed below, because data is sparse on the thermal evolution of the Miechów Trough. However, a recently published paper, on the application of palynofacies analysis and the Thermal Alteration Index (TAI) to determine the degree of organic matter thermal maturity in the Upper Permian and Triassic deposits in the northern part of the Miechów Trough, gave new insights into the thermal evolution of the study area (Fijałkowska-Mader, 2020). In the Upper Permian formations, the VR values are in the range of 0.47–0.90% (Grotek, 2000, 2008; Fijałkowska-Mader, 2020). In the Triassic strata, VR varies within limits of 0.2–0.6% (Fijałkowska-Mader, 2020) and is slightly lower than the value 0.5–1.1% reported by Grotek (2000, 2008). In the Miechów Trough, the relatively low

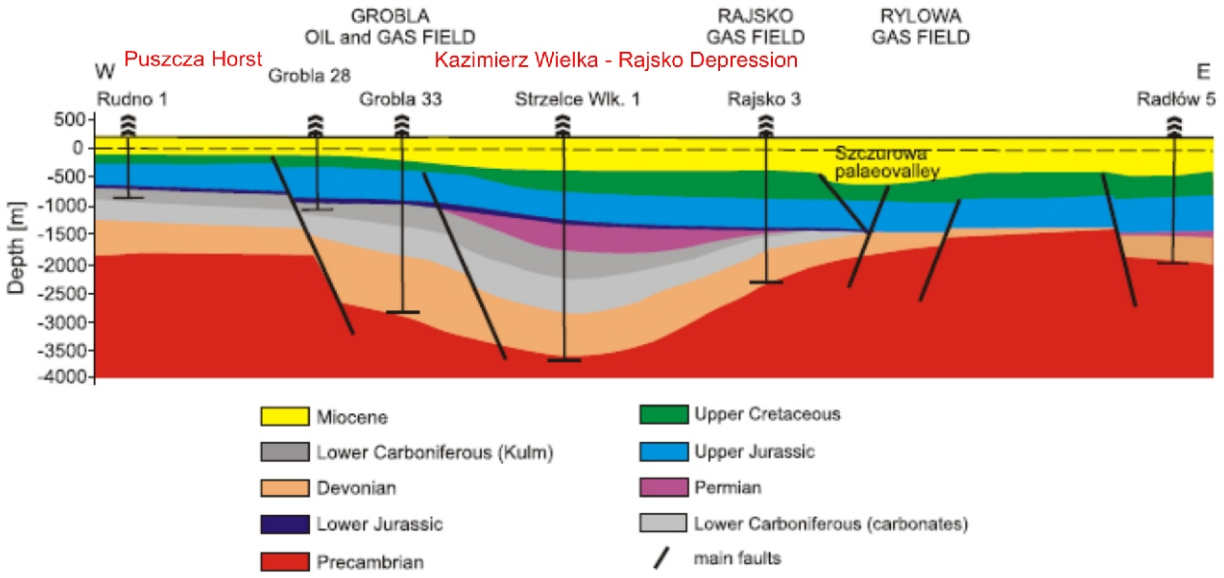


**Fig. 2. Simplified cross-section through the southern part of the study area (after Dudek et al., 2003; Florek et al., 2006)**

conodont CAI values of 1 in the Triassic rocks indicates that the Paleozoic strata must have reached their thermal maturity, of CAI 2–4.5, earlier, most likely in the late Carboniferous (Malec, 2015). Such low values of thermal maturity indicators indicate relatively low diagenesis temperatures (generally <100°C) in the Mesozoic succession of the study area and much higher temperatures in the Paleozoic strata.

Generally, because the Paleozoic-Cenozoic development of the Miechów Trough is similar to that of the HCM area or at least the southern part of it, i.e. the Kielce Unit, the thermal evolution of both areas is similar. In the HCM most authors agree about the key role of the Holy Cross Fault (HCF) in controlling the Variscan thermal regime within the region (Bełka, 1990; Marynowski et al., 2002; Poprawa et al., 2005) and enhancing Carboniferous-Permian advective heat flow through fluid migration (Migaszewski and Hałas,1996; Poprawa et al., 2005; Narkiewicz et al., 2010; Naglik et al., 2016). In the HCM, burial and exhumation events of different magnitudes can be related to HCF polyphase activity. In particular, Variscan deformation in the late Carboniferous (e.g., Lamarche et al., 2003a; Narkiewicz, 2007) was potentially capable of producing a tectonic overburden which might have led to temperature increase and changed organic thermal maturity. In the HCM, thermal maturity distribution data in the pre-Permian versus younger strata points to a prominent role of late Paleozoic heat flow (Bełka, 1990; Narkiewicz et al., 2010; Malec, 2015; Narkiewicz, 2017). A late Variscan cooling event affecting Paleozoic sequences, recorded by zircon helium ages (Botor et al., 2018), marks the end of an important thermal overprint related to Variscan tectonic development (e.g., Lamarche et al., 1999, 2003a; Konon, 2006, 2007). This event may have been triggered by increased heat flow that was, at least partly, coupled with fluid circulation along the HCF (e.g., Narkiewicz et al., 2010). During the Mesozoic, due to sedimentary burial, the increase in temperature across most of the HCM reveals subsidence of the Mid-Polish Trough. The middle part of the HCM (on both side of the HCF, in the Kielce and Łysogóry Units) records a rapid cooling event related to tectonic inversion of the Polish Basin (e.g., Dadlez et al., 1995; Krzywiec, 2002; Lamarche et al., 2003a, b; Scheck-Wenderoth et al., 2008), that started in the Cenomanian to early Campanian (~100–90 Ma in Łysogóry, ~90 Ma, in the Kielce Unit, Botor et al., 2018; ~82–91 Ma in Radwanów IG 1 profile, Łuszczak et al., 2020). This rapid rate cooling is also emphasized by a small time lag between apatite fission-track (109 Ma) and apatite helium ages (91 Ma) in the same surface samples (Dębniak) from the central part of the HCM (Botor et al., 2018). However, tectonic inversion was much less obvious along the SW margin of the HCM (i.e. Kowala and Ostrówka area), where slow cooling took place throughout the Mesozoic with only a minor cooling rate acceleration from the latest Cretaceous (Botor et al., 2018). The NE Mesozoic cover of the HCM also shows a dominance of slow cooling in the late Mesozoic to Paleogene (Cattò, 2014). Therefore, it seems that in the Miechów Trough located much farther towards west, no significant tectonic inversion occurred during the Late Cretaceous-Paleogene. In the Kowala outcrop section (SW HCM), the early mature character of the organic matter indicates maximum burial temperatures lower than 80°C (Bełka, 1990). Low maturity is corroborated by vitrinite reflectance values of ~0.50–0.55% VR (Marynowski et al., 2001), the temperature of maximum release of hydrocarbons (Joachimski et al., 2001; Marynowski et al., 2007, 2010) as well as the conodont CAI index (Joachimski et al., 2001). However, based on smectite illitization, the temperature was estimated at ~130°C (Środoń and Trela, 2012). Therefore, there is a significant discrepancy between the maximum temperature estimated from organic and mineral indices. Inconsistencies between smectite illitisation data and those from organic matter are common. A similar pattern is seen in Ediacaran rocks of the East European craton (Derkowski et al., 2021). Since zircon helium ages for a bentonite horizon in the Kowala section are reset, this was considered as evidence of local short-term hydrothermal fluid flow, which did not change the thermal maturity of the organic matter, but influenced the mineral record of these rocks (Botor et al., 2018). Although illite K-Ar ages from the Kowala exposure were estimated by Zwing (2003) in the range of 315–292 Ma, Środoń and Trela (2012) published illite K-Ar ages in the range of 192 to 228 Ma, supporting a Jurassic diagenetic overprint. Assuming maximum heating only in the Cretaceous as was proposed by Schito et al. (2017) did not give any good results for the

thermochronological dataset (Botor et al., 2018). An alternative model proposed by many authors (e.g., Bełka, 1990; Narkiewicz, 2002; Narkiewicz et al., 2010; Botor et al., 2018) proposes that the main heating interval of the Devonian to early Carboniferous sedimentary successions occurred in the late Carboniferous and/or early Permian, except for the Kajetanów area where an additional pre-Triassic thermal event was suggested by Marynowski et al. (2002).

## SOURCE ROCKS IN THE STUDY AREA

Petroleum source rocks in the study area comprise intervals occurring within the Ordovician, Silurian, Devonian and Lower Carboniferous. Due to their low thermal maturity, Mesozoic rocks are not thought to be source rocks despite the fact that some, such as Jurassic strata, contain significant amounts of organic carbon (Kosakowski et al., 2012; Kotarba et al., 2017). Ordovician and Silurian source rocks are an important source of hydrocarbons, both conventional and unconventional, in the East European Craton and in Paleozoic-Mesozoic basement of the Carpathians Foredeep (Pletsch et al., 2010; Więcław et al., 2011, 2012; Kotarba et al., 2017; Botor et al., 2019; Papiernik et al., 2019). In the Holy Cross Mts., Silurian claystones contain up to ~3% TOC (Smolarek et al., 2014, 2017a, b), while claystones of the Lower Carboniferous Zaręby Formation have mean TOC contents of ~2.8% (Malec et al., 2010). However, their thermal maturity is not higher than the oil window zone. In the Kielce region, Schito et al. (2017) also reported TOC contents higher than 1% which, however, are limited to the Silurian and Ordovician rocks of the Bardo syncline and Middle Devonian strata, where the highest TOC values of ~5 and 9% were measured in individual samples. Middle-Upper Devonian and Lower Carboniferous rocks are important sources of hydrocarbons in several areas of the Paleozoic-Mesozoic basement of the Carpathians Foredeep (e.g., Dudek et al., 2003; Kotarba et al., 2017). Geochemical data showed initial TOC in source rocks of the Paleozoic basement of the Carpathian Foredeep to be ~1.2-3.5% for siliciclastic Ordovician and Silurian rocks, 1.2% for Middle-Upper Devonian carbonates and 1.3% for Lower Carboniferous siliciclastic rocks (Więcław et al., 2011). Kerogen type is mainly type II oil-prone low-sulphur in the Ordovician and Silurian rocks, and type II with and admixture of type III in the Middle-Upper Devonian and Lower Carboniferous rocks. The thickness of these source rocks is ~40–50 m for the Silurian and up to 100–150 m for Lower Carboniferous and Ordovician siliciclastic rocks, and up to 200 m for the Devonian succession (Dudek et al., 2003; Więcław et al., 2011; Kotarba et al., 2017). The Upper Jurassic carbonate and the Cenomanian sandstone reservoirs (e.g., in the Grobla, Rajsko, Rylowa and Wierzchosławice oil and gas fields) contain geochemically very similar hydrocarbons. These were generated by thermogenic processes and migrated, probably through fault zones, from source rocks included in the Lower Carboniferous and Middle-Upper Devonian as well as in Ordovician to Silurian strata (Kotarba et al., 2017). However, there is an alternative possibility for the origin of these hydrocarbons. Based on numerical modeling Nemčok and Henk (2006) have shown that it is possible that the hydrocarbons migrated from the Oligocene Menilite Beds of the Outer Carpathians. Moreover, geochemical data also show that oils in the Mesozoic basement are similar to many oils in the Western Outer Carpathians. Some biomarkers such as oleane, derived from angiosperm plants, show that the source rocks for this oils have to include Cretaceous or younger rocks. The high sulphur content in the oils can be related to high sulphur II type kerogen documented in the lower Menilite Beds (ten Haven et al., 1993; Curtis et al., 2004; Lewan et al., 2006). Due to the high sulphur content, such kerogen was able to generate oil much earlier and faster than that of typical low-S-II type (Curtis et al., 2004; Lewan et al., 2006). Recently, Botor (2021) showed that in the frontal Carpathian orogenic wedge, the underlying Paleozoic source rocks attained maximum heating in the Late Triassic to Early Jurassic interval, that triggered a major phase of hydrocarbon generation. The hydrocarbon potential of the Paleozoic source rocks was depleted before the Upper Jurassic and Cenomanian reservoir rocks and traps were formed. Consequently, the majority of the hydrocarbons generated during the pre-Jurassic stages were already dispersed.

## METHODS AND SAMPLES

Mean random VR was analysed in 40 samples from 6 boreholes in the Miechów Trough (Jaronowice IG 1, Milianów IG 1, Pągów IG 1, Potok Mały IG 1, Węgrzynów IG 1, Włoszczowa IG 1), though only 32 samples contained sufficient organic material for effective determination. This dataset has enabled the analysis of thermal maturity versus depth relationships by both basin and stratigraphic interval. Detailed geological information on these boreholes were given by Jurkiewicz (1974, 1975, 1976a, b, 1980, 1990).

## ORGANIC PARTICLE REFLECTANCE MEASUREMENTS

In Devonian and younger strata the thermal maturity of organic matter is widely based on vitrinite reflectance; however, Lower Paleozoic strata do not contain vitrinite. Therefore, thermal maturity in such sediments is based on zooclasts and solid bitumen. In this work 3 Silurian zooclast samples and 29 vitrinite samples were analysed to determine VR (Table 1). The rock samples were cut perpendicular to the bedding and from these rock pieces polished slides were prepared for VR measurements. Mean random VR was measured to determine the thermal maturity of the samples analysed. VR measurements were performed using a Zeiss microscope for incident light, a 50×/0.85 Epiplan–Neofluar oil immersion objective and a 546 nm filter, Zeiss immersion oil $n_e = 1.518$, at a temperature of 23°C. Mineral standards of known reflectance were used for calibration: sapphire (0.590%), yttrium-aluminium garnet (0.901%), gadolinium-gallium garnet (1.718%), cubic zirconium (3.130%) and strontium-titanate (5.390%). The microscopical analyses closely followed the guidelines published by Taylor et al. (1998) and Hackley et al. (2015).

In contrast to the traditional concepts that consider organic maturation as a function of both maximum burial temperature and effective heating time (e.g., Hantschel and Kauerauf, 2009), the time–independent approach (Barker and Pawlewicz, 1994) has obtained general acceptance for reconstructing thermal histories of areas characterized by complex geological histories (e.g., Barker and Pawlewicz, 1994; Tobin and Claxton, 2000; Frings et al., 2004; Cavailhes et al., 2018; Kalinowski and Gurba, 2020). While the application of time–temperature models is limited to sedimentary basins with well-known burial and thermal histories, the time-independent method based on several correlations between VR and maximum temperature can be applied to complex orogenic sequences (e.g., Laughland and Underwood, 1993) and hydrothermal systems (e.g., Barker, 1983). Excellent correlations between fluid–inclusion homogenization temperature and vitrinite reflectance indicate temperature as the major control on organic maturation (e.g.,

Table 1

**Mean random vitrinite reflectance data for the samples from the Miechów Basin**

| Borehole | Depth (m) | Stratigraphy | VR (%) | STD | No | T1 (°C) | T2 (°C) |
|---|---|---|---|---|---|---|---|
| Jaronowice IG 1 | 1367.5 | Bathonian | 0.53 | 0.03 | 51 | 84.3 | 70.9 |
| | 1737.4 | Upper Triassic | 0.64 | 0.03 | 55 | 99.5 | 95.1 |
| | 2005.2 | Emsian | 0.97 | 0.05 | 99 | 133.1 | 148.3 |
| | 2131.4 | Lower Silurian | 1.05 | 0.09 | 63 | 139.4 | 158.4 |
| | 2216.2 | Lower Silurian | 1.00 | 0.04 | 60 | 135.5 | 152.2 |
| Milianów IG 1 | 2276.5 | Visean-Lower Namurian | 2.35 | 0.12 | 138 | 204.4 | 261.4 |
| | 2458.7 | Visean-Lower Namurian | 2.39 | 0.13 | 152 | 205.7 | 263.6 |
| | 3220.1 | Visean-Lower Namurian | 3.06 | 0.11 | 100 | 225.7 | 295.2 |
| Pągów IG 1 | 587.5 | Coniacian-Turonian | 0.56 | 0.07 | 86 | 88.7 | 78.1 |
| | 1469.2 | Bajocian | 0.62 | 0.07 | 100 | 96.9 | 91.1 |
| | 1501.6 | Lower Jurassic | 0.65 | 0.09 | 110 | 100.7 | 97.1 |
| | 1887.1 | Upper Triassic | 0.70 | 0.07 | 100 | 106.7 | 106.6 |
| | 2593.1 | Zechstein | 1.11 | 0.08 | 100 | 143.9 | 165.5 |
| | 2664.2 | Visean | 2.88 | 0.14 | 82 | 220.8 | 287.4 |
| | 2780.2 | Visean | 2.88 | 0.14 | 80 | 220.8 | 287.4 |
| | 2995.8 | Famennian | 2.99 | 0.13 | 62 | 223.8 | 292.2 |
| Potok Mały IG 1 | 1608.5 | Upper Triassic | 0.64 | 0.04 | 78 | 99.5 | 95.1 |
| | 1700.0 | Upper Triassic | 0.82 | 0.07 | 98 | 119.5 | 126.8 |
| | 1789.0 | Lower Triassic | 1.00 | 0.06 | 56 | 1350 | 1520 |
| Węgrzynów IG 1 | 1070.4 | Visean | 0.66 | 0.05 | 102 | 101.9 | 99.1 |
| | 1369.7 | Visean | 0.70 | 0.04 | 78 | 106.7 | 106.6 |
| | 1549.7 | Famennian | 0.85 | 0.08 | 77 | 122.4 | 131.4 |
| | 2175.9 | Frasnian | 0.99 | 0.08 | 69 | 134.7 | 150.9 |
| | 2447.4 | Frasnian | 1.20 | 0.08 | 57 | 150.2 | 175.5 |
| | 2524.2 | Givetian | 1.56 | 0.09 | 86 | 171.4 | 209.4 |
| | 3015.7 | Eifelian | 2.75 | 0.08 | 91 | 217.1 | 281.5 |
| Włoszczowa IG 1 | 955.5 | Kimmeridgian | 0.49 | 0.04 | 55 | 77.9 | 60.9 |
| | 1593.6 | Bathonian | 0.52 | 0.03 | 64 | 82.7 | 68.6 |
| | 1615.9 | Bathonian | 0.53 | 0.05 | 72 | 84.3 | 70.9 |
| | 2147.5 | Upper Triassic | 0.77 | 0.06 | 53 | 114.4 | 118.7 |
| | 2251.1 | Middle Triassic | 0.80 | 0.07 | 58 | 117.5 | 123.6 |
| | 2594.6 | Silurian | 0.92 | 0.09 | 62 | 128.6 | 141.5 |

VR (%) – mean random vitrinite reflectance, STD – standard deviation, No – number of measurements per sample, T1 – maximum temperature calculated from VR data for burial model (Barker and Pawlewicz, 1994), T2 – maximum temperature calculated from VR data for hydrothermal model (Barker and Pawlewicz, 1994)

Barker and Pawlewicz, 1994; Tobin and Claxton, 2000). VR was used as an input parameter for the calculation of peak temperature after Barker and Pawlewicz (1994). In the present study, the formula Temperature 1 = (lnVR + 1.68)/0.0124 for the burial heating model and Temperature 2 = (lnVR + 1.19)/0.00782 for the hydrothermal heating model after Barker and Pawlewicz (1994) was applied. The formulas are calibrated up to 7% VR (Barker and Pawlewicz, 1994).

## PETROMOD MODELING TECHNIQUE

Thermal maturity modeling was performed using the 1-D *PetroMod* software (Schlumberger, ver. 9.0; for details see Hantschel and Kauerauf, 2009). The numerical modeling techniques applied enabled the simulation of the complex set of interacting physical and chemical processes that took place during the evolution of the sedimentary basin. The beginning point for the modeling is a conceptual model (Waples et al., 1992a, b; Hantschel and Kauerauf, 2009), which identifies the geological evolution of the study area, including geological, geophysical, and geochemical data. A discretized numerical model, which represents the conceptual model, is then applied for simulation purposes (Waples et al., 1992a, b; Hantschel and Kauerauf, 2009). The geological history of an individual borehole section is calculated using the finite difference method. Stratigraphic events, scaled in time, establish the structure of the model and control the data input. The data set for each event consists of duration, depositional or erosional thickness, lithology, bathymetry, sediment/water interface or surface temperature, heat flow and rock thermal properties. Petrophysical parameters, such as porosity, density and thermal conductivity, are then classified on the basis of lithology. After each simulation run, the calculated results are compared with the measured values to calibrate the model and test its geological consistency. Calibration is usually performed by varying the palaeo-heat flow or the original thickness of the now-eroded sedimentary units (Waples et al., 1992a, b; Hantschel and Kauerauf, 2009). Initially, heat flow estimates for the past stages of basin evolution are given on the basis of the tectonic setting (Hantschel and

Table 2

**Input data for the Włoszczowa IG 1 model**

| Event / stratigraphy | Top (m) | Bottom (m) | Thick-ness (m) | Erosion (m) | Deposition | | Erosion | | Lithology |
|---|---|---|---|---|---|---|---|---|---|
| | | | | | from (Ma) | to (Ma) | from (Ma) | to (Ma) | |
| Quaternary | 0.00 | 10.00 | 10.00 | | 2.00 | 0.00 | | | SILTSTONE |
| Paleogene-Neogene | 10.00 | 10.00 | 0.00 | | 55.00 | 2.00 | | | none/hiatus |
| Maastrichtian | 10.00 | 303.00 | 293.00 | 200.00 | 72.00 | 65.00 | 65.00 | 55.00 | MARL |
| Campanian | 303.00 | 620.00 | 317.00 | | 83.00 | 72.00 | | | MARL |
| Santonian | 620.00 | 726.00 | 106.00 | | 86.00 | 83.00 | | | MARL |
| Coniacian | 726.00 | 780.00 | 54.00 | | 89.00 | 86.00 | | | MARL |
| Cenomanian | 780.00 | 839.00 | 59.00 | | 100.50 | 89.00 | | | SANDSTONE |
| Albian | 839.00 | 850.00 | 11.00 | | 113.00 | 100.50 | | | SANDsilty |
| Kimmeridgian | 850.00 | 1060.00 | 210.00 | 400.00 | 157.00 | 145.00 | 145.00 | 113.00 | LIMESTONE |
| Oxfordian | 1060.00 | 1613.00 | 553.00 | | 163.00 | 157.00 | | | LIMESTONE |
| Bathonian | 1613.00 | 1631.00 | 18.00 | | 168.00 | 163.00 | | | SILT&SAND |
| Bajocian | 1631.00 | 1667.00 | 36.00 | | 170.00 | 168.00 | | | SILT&SAND |
| Lower Jurassic | 1667.00 | 1703.00 | 36.00 | | 201.00 | 170.00 | | | SANDSTONE |
| Upper Triassic | 1703.00 | 2338.00 | 635.00 | | 237.00 | 201.00 | | | SILTsandy |
| Permian | 2338.00 | 2338.00 | 0.00 | | 275.00 | 250.00 | | | ANHYDRITE |
| Visean-Namurian | 2338.00 | 2338.00 | 0.00 | 500.00 | 345.00 | 315.00 | 315.00 | 275.00 | SAND&SILT |
| Upper Devonian | 2338.00 | 2338.00 | 0.00 | 800.00 | 382.00 | 359.00 | 359.00 | 345.00 | LIMEdolom |
| Givetian | 2338.00 | 2512.00 | 174.00 | | 387.70 | 382.00 | | | LIMESTONE |
| Emsian | 2512.00 | 2541.00 | 29.00 | | 407.60 | 387.70 | | | SANDsilty |
| Silurian | 2541.00 | 2618.00 | 77.00 | 100.00 | 425.00 | 419.00 | 419.00 | 408.00 | SILTSTONE |

In lithology types the following system was applied for abbreviations: e.g., SANDsilty (first lithology in upper case and second in lower case) means 70% sandstone and 30% of siltstone; SILT&SAND (both lithologies in upper case) – 50% siltstone and 50% sandstone, petrophysical properties of lithology is given in Botor (2023)

Kauerauf, 2009). In the subsequent iterations, the palaeoheat flow values are modified through the modeling procedure to achieve the best fit between the calculated model and the measured calibration parameters. Heat flow values are the best constrained for timing of the maximum temperature, which usually links to the maximum sedimentary burial (Hantschel and Kauerauf, 2009). The backstripping method, which also includes a decompaction correction, was applied to establish the burial history. Petrophysical parameters were used based on the PetroMod library according to lithological types identified in the boreholes analysed (Botor, 2023). Models were calibrated using measured values of mean random vitrinite reflectance. The VR in modeling was calculated using the algorithm of Sweeney and Burnham (1990). Several tests of the change of heat flow over time, erosion/exhumation of overburden, and a combination of both, were performed. The calculated VR values were compared with the measured VR values, and the computer model was adjusted until the best fit of the VR versus depth was achieved. A broader discussion of the applied maturity modeling method is provided elsewhere (Waples et al., 1992a, b; Hantschel and Kauerauf 2009).

## INPUT DATA IN MODELING

Among the six borehole available for this study, only Włoszczowa IG 1, Jaronowice IG 1 and Pągów IG 1 have VR data from both the Paleozoic and Mesozoic parts of the stratigraphic section (Table 1). However, Włoszczowa IG 1, located in the central part of the study area, is representative of the Miechów Trough. In the Włoszczowa IG 1 borehole section, the VR dataset included six samples from the Mesozoic and Paleozoic strata (Table 1). While developing a numerical model, a great number of uncertainties have to be discussed and evaluated. Major variables that influence the basin model are related to petrophysical properties of the basinal deposits, mode of heat transfer, calibration data and the algorithm for the VR data (Waples et al., 1992a, b; Hantschel and Kauerauf, 2009). During this study it was not possible to measure the thermal conductivity or heat capacity of the basin deposits due to sparse sample material. Therefore, these values were quantified for all formations by combinations of default rock property data with respect to borehole descriptions. The surface palaeotemperature was set automatically using the SWIT tool, which extracts a standard temperature at sea level over geological time for any given location, based on the model of Wygrala (1989). The present-day surface average temperature is assumed to be 9°C. We did not consider the palaeo-water depth because the predominant influence on the thermal evolution is exerted by stratal thickness, as most of the sedimentation in the study area occurred in shallow water platform environments that did not exceed 200 m (Jurkiewicz, 1975).

The stratigraphic section of the Włoszczowa IG 1 borehole is shown in Table 2. In the section, a significant stratigraphic unconformity occurs between the Givetian (Devonian) and Lower Triassic strata (Table 2). The next important unconformity occurs between the Upper Jurassic and the Lower/Upper Cretaceous, and between the Upper Cretaceous and Miocene. These gaps in the sedimentary record allow different hypotheses to be inferred regarding the burial history of the study area, as discussed below. Geothermal gradients in the boreholes analysed range between 23 and 30°C/km. In the study area the average present-day surface heat flow is in the range of ~50–60 mW/m$^2$ (e.g., Majorowicz et al., 2019 and the references therein). In Włoszczowa IG 1, heat flow was calculated at 54 mW/m$^2$ based on temperature data from Jurkiewicz (1990).

## RESULTS

In the boreholes analysed, VR values vary from 0.49 to 3.06% and increase with depth (Table 1). The number of VR measurements per sample range from 51 to 152, and standard deviation is low, usually below 0.1. Only samples having mean VR values above 2.0% have a higher standard deviation (up to 0.14). Estimated maximum palaeotemperatures of the rocks analysed based on VR values range from 78 to 225°C for a burial-induced model and from 71 to 295°C for a hydrothermal-induced model (Table 1; Barker and Pawlewicz, 1994).

In general, VR data from the Paleozoic and Mesozoic sections of the Miechów Trough are defined as having low scatter, and show some trends reflecting the thermal evolution of the study area. This allows interpretation of VR profiles to characterize the thermal history and the prevalent heat transfer mechanisms within the basin. Calculated peak palaeotemperatures from the boreholes are used to compute palaeogeothermal gradients and to estimate the magnitude of net exhumation at selected locations. The measured VR values were plotted on a logarithmic scale which allowed estimatation of the thermal maturity gradient and the maximum thickness of the overburden (Yamaji, 1986; Connolly, 1989; Frings et al., 2004). Assuming that the palaeo-surface vitrinite (huminite) reflectance was ~0.25%VR (equivalent to a palaeo-surface temperature of ~25°C), the intersection of the regression line at this point can be used to predict the maximum overburden (Fig. 3).

In the Pągów IG 1 borehole, VR values change from 0.56% in the Albian-Maastrichtian strata to 1.11% in the bottom of the Zechstein, whereas in Visean-Upper Devonian strata organic matter is overmatured, having VR values in the range 2.88–2.99% (Fig. 3A). There is obvious jump in VR values between the Visean-Upper Devonian and Permian-Mesozoic sections. The VR data allows estimation of post-Cretaceous erosion to 1800 m, and post-Variscan erosion as 1100 m. In particular, the post-Cretaceous exhumation seems to be too high considering the mild tectonic inversion in the Miechów Trough. In the Milianów IG 1 borehole, VR of 0.47–0.56% in the Zechstein strata were noted by Grotek (2018). In the Triassic strata, a VR value of 0.78% was measured (Grotek, 2018). Such decrease from Triassic into Zechstein can be attributed as fluid flow influence. In Visean strata of the Milianów IG 1 borehole, VR values are in the range 2.35 to 3.06%, comparable to those of the Pągów IG 1 (Fig. 3B). Therefore, a VR break is inferred in this section. Post-Variscan erosion needs to be taken as 6000 m; otherwise, a fluid flow event should be assumed.

Towards the south of the Miechów Trough the next borehole analysed is Jaronowice IG 1, in which VR values are in the range from 0.53% in the Bathonian-Kimmeridgian to 1.05% in the Emsian-Eifelian (Fig. 3C). However, the Ordovician-Silurian shows decreasing vitrinite-like reflectance, to 1.0 and 0.98%. Because the bottom of the Triassic shows VR of 0.64%, and the Devonian below 0.97%, a VR break is inferred as in the two previous boreholes (Pągów IG 1 and Milianów IG 1). In the Potok Mały IG 1 borehole only a few VR samples were obtained; from 0.64 to 0.82 % in the Triassic strata. These data are from the depth interval of 1600–1800 m, suggesting the probable influence of hot fluids (Fig. 3D). In the Węgrzynów IG 1 borehole, VR data range from 0.66% in the Visean to 2.75% in the Eifelian (Fig. 3E). There is no evident VR jump between Carboniferous and Devonian. However, the slightly dispersed and not fully linear VR pattern might be related to overpressure development (Fig. 3E). In the Włoszczowa IG 1 borehole, VR values are from 0.49% in the Kimmeridgian to 0.92% in the Silurian and do not shows any breaks (Fig. 3F). A similar value 0.84% VR for Triassic strata was also recorded by Grotek (2018).

In the following step VR values were used as an input parameter for the estimation of maximum palaeotemperature after Barker and Pawlewicz (1994) approach. By plotting these calculated temperatures against depth, palaeogeothermal gradients for the time of the highest temperatures in the basin can be also calculated (Fig. 4). These calculation are based on assumption that thermal conductivity of exhumed rocks is the same as preserved in the section analysed (Yamaji, 1986; Connolly, 1989; Frings et al., 2004).

Considering all the boreholes analysed, the linear increase of present-day temperature shows an average geothermal gradient of 24°C/km with individual boreholes ranging from 23 to 30°C/km (Fig. 4). Generally, palaeotemperatures in the boreholes analysed show that it was hotter in the past than today. Palaeogeothermal gradients were varied in the Mesozoic and Paleozoic. In the Pągów IG 1 borehole, the Zechstein-Mesozoic section shows a palaeogeothermal gradient of 23°C/km, which is lower than the present-day one of 30°C/km (Fig. 4A). However, for a hydrothermal-induced model, a palaeogeothermal gradient of 43°C/km was calculated. Very high temperatures (>200°C) calculated in the Pagów IG 1 borehole lead to an overestimation of the estimated Variscan erosion to over 10 km – an unrealistic value. In the Milianów IG 1 borehole, the Carboniferous section shows a paleogeothermal gradient of 22°C/km for a burial-induced model and ~36°C/km for a hydrothermal-induced model (Fig. 4B). Estimated Variscan erosion is also very high (>8 km). In the Jaronowice IG 1 borehole, the Mesozoic section suggests erosion ~800 m, and a palaeogeothermal gradient of 41°C/km for a burial-induced model and ~65°C/km for a hydrothermal-induced model (Fig. 4C). In the Potok Mały IG 1 borehole, VR-based data shows a palaeogeothermal gradient of 200°C/km for a burial-induced model and ~316°C/km for a hydrothermal-induced model that occurred after Triassic (Fig. 4D). Such high values seem to be unrealistic and strongly suggest hydrothermal fluid influence on the thermal maturity of the organic matter. In the Węgrzynów IG 1 borehole, VR-based data shows a palaeogeothermal gradient of 59°C/km for a burial-induced model and 94°C/km for a hydrothermal-induced model (Fig. 4E). These data suggest Variscan erosion of ~2000 m; however, this pattern of data in the borehole suggests fluid flow influence in the Late Paleozoic. In the Włoszczowa IG 1 borehole, VR-based data shows a palaeogeothermal gradient of 31°C/km for a burial-induced model and 50°C/km for a hydrothermal-induced model in the Mesozoic with post-Jurassic erosion amounting to 800 m (Fig. 4F). Because Upper Cretaceous strata are documented up to the Maastrichtian, such an erosion event was related rather to the latest Jurassic section. In the Lower to Middle Jurassic section lower VR values were observed. Such a pattern can be attributed to a fluid flow event.

During thermal modeling by means of *PetroMod* software, several models were tested; among these, only a few are shown to illustrate the most prominent scenarios (Fig. 5). The first model for the Włoszczowa IG 1 borehole (1) assumed a heat flow of 62 mW/m$^2$, constant in time, which is the average value for the crust (Allen and Allen, 2005). Exhumation was assumed as the following: Upper Cretaceous 300 m, Upper Jurassic 400 m, Late Devonian 700 m, and Carboniferous 500 m. Such estimates represent typical values accepted in adjacent areas (e.g., Narkiewicz et al., 2010; Łuszczak et al., 2020). In the second model (2) heat flow was assumed as 60 mW/m$^2$ from the Silurian to the end of the Cretaceous, and adjusting in the Cenozoic to the present-day value of 54mW/m$^2$. All other parameters were left the same as in model 1. Both models 1

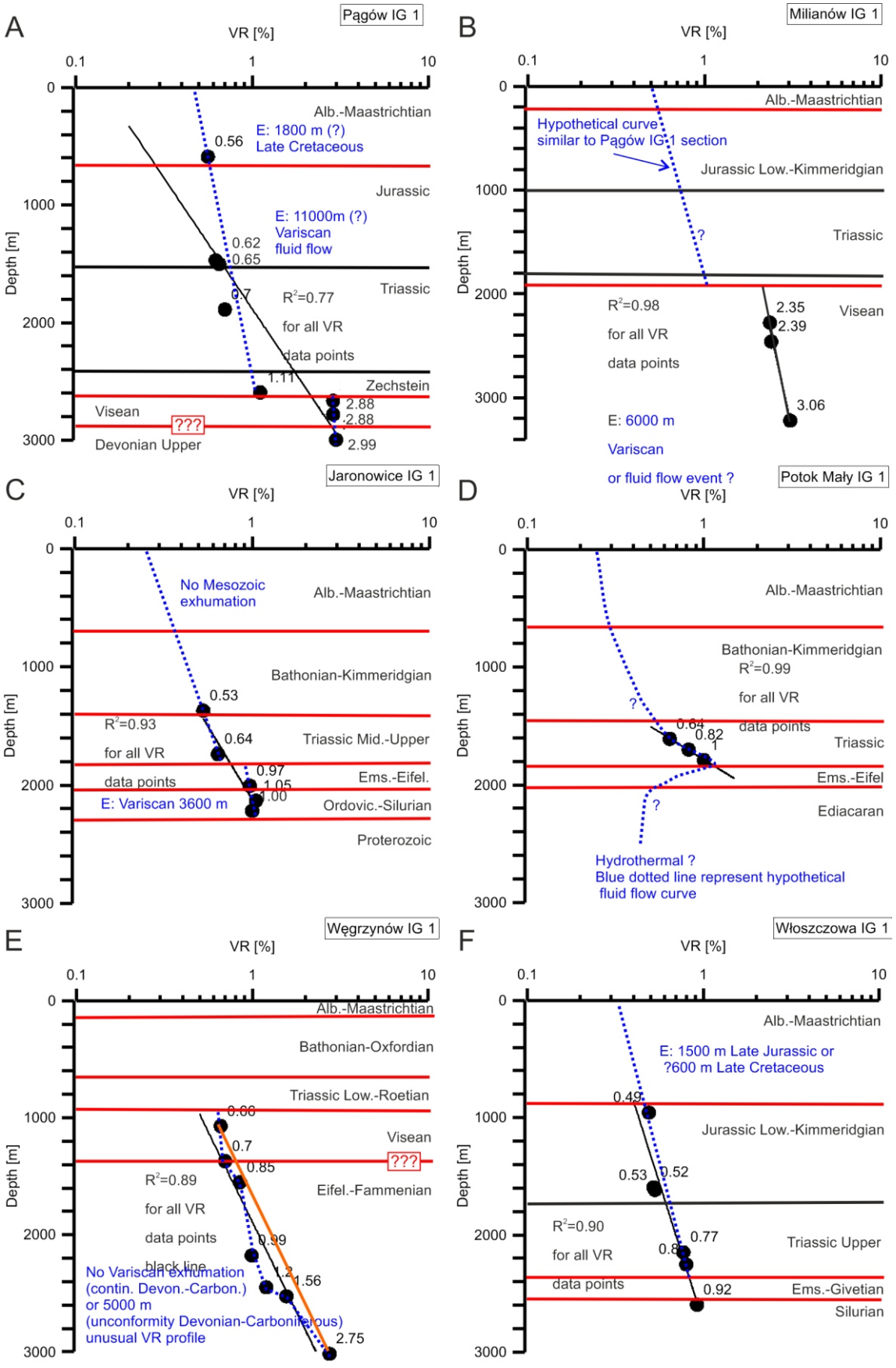


**Fig. 3. Depth vs. vitrinite reflectance profiles in the study area of the Miechów Trough**

Stratigraphy based on Jurkiewicz (1974, 1975, 1976a, b, 1980, 1990). This analysis assumes that the thermal conductivity of the eroded sequences was the same as that of the preserved sequences. Red horizontal line represents unconformity. Black horizontal line represents continuous section. Assumed initial VR value is 0.25%

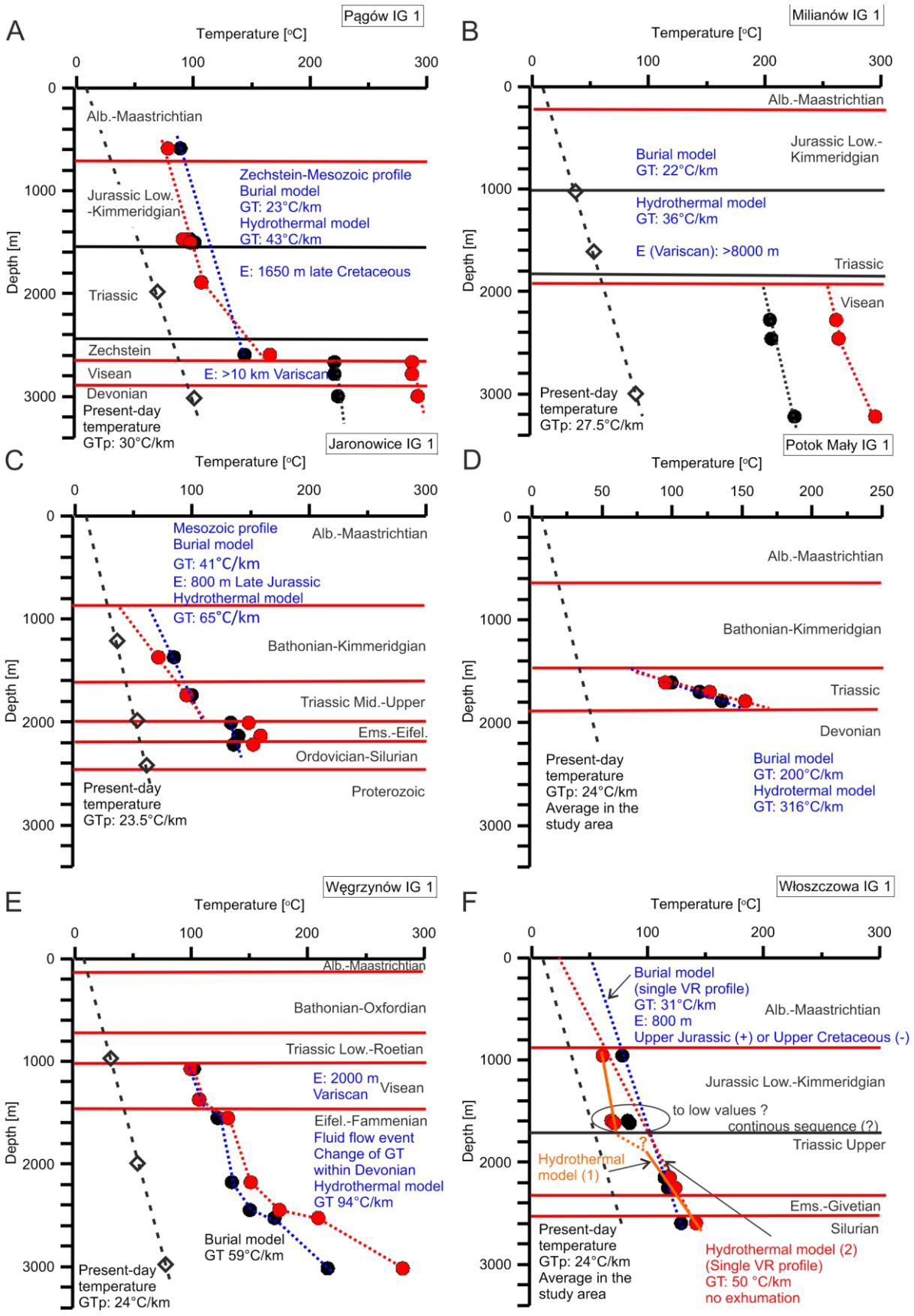


**Fig. 4. Fluid flow driven palaeotemperature profiles in the study area**

Palaeotemperature values are calculated based on Barker and Pawlewicz (1994): black dots – burial model; red dots – hydrothermal model. Fluid flow-driven shape of palaeotemperature curves is based on Ziagos and Blackwell (1986). Present-day temperature data from Jurkiewicz (1975, 1990). GTp – present-day geothermal gradient. GT – palaeogeothermal gradient, E – exhumation/erosion

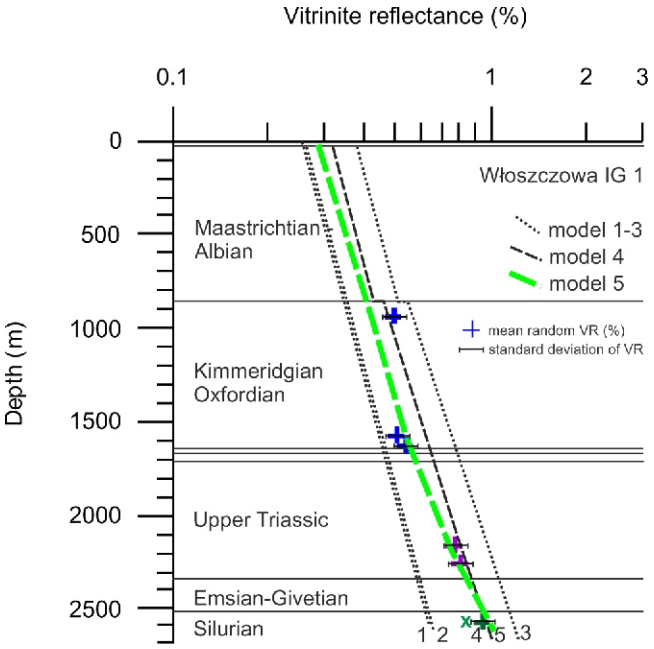


**Fig. 5. The mean vitrinite reflectance data vs. calculated models for the Włoszczowa IG 1 borehole section**

The first model (1) assumed heat flow (HF) 62 mW/m$^2$ constant in time. Exhumation: Upper Cretaceous 300 m, Upper Jurassic 400 m, Late Devonian 700 m, and Carboniferous 500 m. In model (2) HF is assumed as 60 mW/m$^2$ up to the end of Cretaceous and then adjusting to the present-day value of 56 mW/m$^2$. All other parameters were left the same as in model 1. In model (3) Upper Jurassic erosion was increased to 1300 m. In model (4) Upper Jurassic exhumation was decreased to 1100 m. Finally in model (5) extremely high HF was assumed at 140 mW/m$^2$ in Middle to Late Jurassic times in order to simulate a hot fluid flow event and Upper Jurassic erosion was assumed to 450 m. All others parameters were kept without changes. This last model is considered as the best-fit model. Lithology of exhumed rocks applied in all models: Upper Cretaceous – chalk, Upper Jurassic – Limestone 70% and marls 30%, Carboniferous – sandstone70%/shale 30%, Devonian – Limestone70%shale30%

and 2 show calculated VR values too low by comparison with the measured ones. The VR data in this borehole include samples from the Silurian to the Kimmeridgian. Thus, the major event that influenced the thermal maturity pattern in this borehole needs to be Middle-Late Jurassic or post-Jurassic, particularly for the Mesozoic section. Therefore, in model (3), Late Jurassic erosion increased to 1300 m. Such high values were also accepted as the maximum values possible for the Late Jurassic by Łuszczak et al. (2020). Unfortunately, this model gave overestimation of the VR. In the next model (4), Late Jurassic exhumation decreased to 1100 m. Such a model gave a reasonably good fit of measured vs. calculated VR values, except for two Oxfordian values. However, 1 km of eroded Upper Jurassic deposits included the Oxfordian to Tithonian strata (Łuszczak et al., 2020). In the case of Włoszczowa IG 1, Oxfordian to Kimmeridgian strata occur in the section. Therefore, such a high value of Late Jurassic erosion seems to be an overestimate. Therefore, finally in model (5), extremely high heat flow was assumed as 140 mW/m$^2$ in Middle-Late Jurassic times in order to simulate a hot fluid flow event (Fig. 5). Upper Jurassic exhumation was lowered to 450 m. All other parameters were kept without changes. This last model is thought to be the preferred best-fit model and is presented as the ultimate model (Fig. 6). In this model, increase of temperature occurred after deposition of the youngest sampled interval. The growth of temperature and thermal maturity in the Włoszczowa IG 1 borehole profile took place mainly during the Middle to Late Jurassic (Fig. 7). Because high values of Late Jurassic erosion cannot be inferred, the only possibility to explain the distribution of VR in this section is to assume a Middle Jurassic hydrothermal event.

During the numerical modelling it became obvious that varying only single input data in the models would not provide an acceptable fit. Consequently a number of different combinations of parameters, such as the maximum subsidence, or the variation of the maximum heat flow values and their duration were considered in numerous model iterations to determine the scenario with the best fit to the thermal maturity data. However, as can be seen in Figure 5, there is no perfect thermal model, that might be able to fully satisfy all measured VR data in a given borehole section in the study area. The major reason for

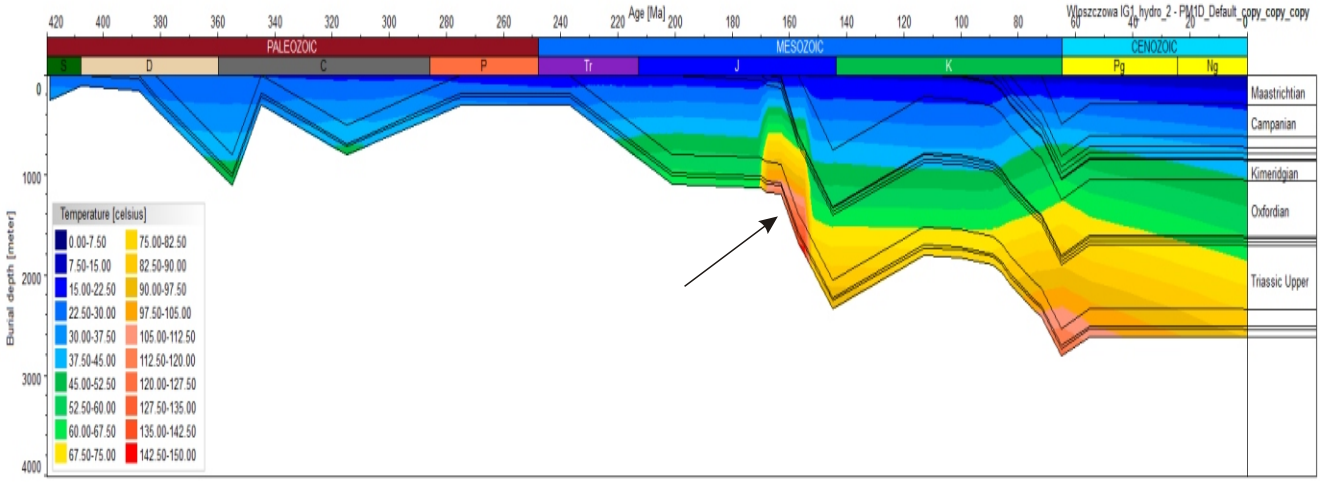


**Fig. 6. Burial and thermal history model for the Włoszczowa IG 1 borehole**

VR calibration was shown in Figure 5. HF in Mid-Late Jurassic was assumed as 140 mW/m$^2$. Such a too-high HF value, considering the tectonic setting of the study area, suggests a hot fluid flow event. See further explanation in the text

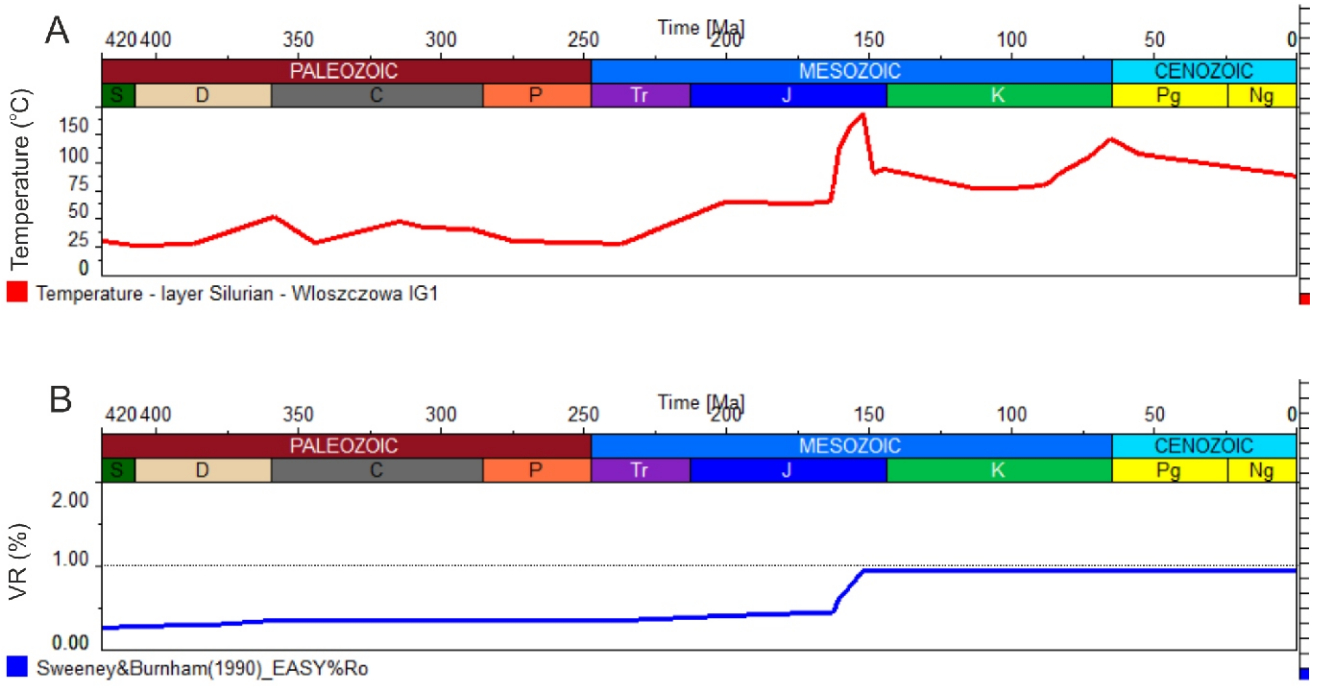


**Fig. 7. Temperature (A) and vitrinite reflectance (B) for the top of the Silurian strata in the Włoszczowa IG 1 model**

The results of the best-fit model are shown (model 5 from Fig. 5). Maximum increase of temperature in the Late Jurassic caused increase of vitrinite reflectance up to the level measured today (0.92% VR, see Table 1). Further explanation in the text

this is the nature of heat transfer in the sections analysed, that is fluid flow-driven diagenesis. The software applied calculated only a conductive model of heat transport, whereas in the Miechów Basin advective heat transport, mediated by fluids, was the most important factor. The non-linear VR pattern in the sedimentary successions analysed strongly support the idea that lateral fluid flow events occurred in the Miechów Trough.

## DISCUSSION

Empirically derived methods of calculating peak palaeotemperature from VR (e.g., Barker and Pawlewicz, 1994) are compared with computer kinetic models (PetroMod results for Włoszczowa IG 1 borehole; Easy%Ro, Sweeney and Burnham, 1990) and, although differing in detail, within the resolution of this dataset are shown to produce similar trends. Lateral variations between boreholes in palaeogeothermal gradients based on VR data recorded in the Paleozoic and Mesozoic sections of the Miechów Trough seem consistent with a gravity-driven hydrothermal system discharging heated fluids (e.g., Lampe et al., 2001; Tóth, 2009; Incerpi et al., 2020). Generally, the timing of hydrothermal fluid flow is difficult to constrain because of the multi-stage flow history of the fracture pathways, although potential periods of hot fluid flow in the Miechów Trough include Late Devonian-Lower Carboniferous, Late Carboniferous-Early Permian, Triassic and Jurassic times, and Late Cretaceous to Paleogene. In general, palaeogeothermal gradients are substantially higher in the Paleozoic sections than in the Mesozoic sections (Fig. 4). The thermal maturity of organic matter dispersed in the Lower Paleozoic to Mesozoic sedimentary successions is in the range of 0.49 to 3.06% of VR. The estimated maximum palaeotemperatures of the rocks analysed range from ~70 to ~290°C. The Variscan thermal regime was different from the Mesozoic one. At least two fluid flow events might be identified. The maximum palaeotemperature (~120–290°C) in the Silurian to Lower Carboniferous sedimentary succession was achieved in the late Carboniferous to early Permian. The Late Variscan tectonic activity may have been triggered by increased heat flow that was, at least partly, coupled with fluid circulation. The maximum palaeotemperature (~70–150°C) of the Zechstein to Jurassic sedimentary succession was achieved during the Middle to Late Jurassic. It was likely caused by a hot fluid flow event. Thermal maturation levels of the Paleozoic sections are considered to be the consequence of burial, elevated heat flow and a regional advective system developed during late Carboniferous to early Permian times rather than Mesozoic or Cenozoic processes, similarly as in the HCM (Botor et al., 2018). In the Middle Jurassic, there was likely a second fluid flow event that caused thermal maturation of the Zechstein and Triassic to Jurassic strata. Such a Jurassic hydrothermal event has been suggested earlier in the central part of the Polish Basin (Kozłowska and Poprawa, 2004, Zieliński et al., 2012; Kuberska et al., 2021). Therefore, it seems that such fluid flow processes have a wider extent, including in the Miechów Trough.

In the HCM carbonate veins are widely known and five phases have been distinguished: A – Variscan (Visean/Namurian), B – older post-Variscan (post-Namurian through pre-Zechstein), C and D – younger post-Variscan (Permian/Triassic and middle/late Early Triassic), and E and F - Cimmerian-Alpine (Late Jurassic and Late Cretaceous) (e.g., Migaszewski and Hałas, 1996). These veins are related to polyphase fluid flow events. However, the Jurassic hydrothermal events in particular, present across all central and Western Europe, are linked to far-field stress changes related to both Tethys and Atlantic rifting (e.g., Timar-Geng et al., 2004; Bossennec et al., 2021). The Upper Jurassic deposits in the substrate of the Carpathian Foredeep shows that there is a complete Late Jurassic succession (Matyja 2009). However,

the thickness of the Oxfordian and Kimmeridgian succession is twice to three times smaller than previously assumed (Matyja, 2009). Therefore, a significant Late Jurassic to Early Cretaceous exhumation is impossible. Indeed, in the Mesozoic history of the SE part of the Mid-Polish Trough several phases of tectonic extension were identified, from Triassic/Early Jurassic to Kimmeridgian, which were related mainly to the Holy Cross Fault. Extension with dextral movement along the Zawiercie Fault was also found from the Kimmeridgian to Early Albian (Gutowski and Koyi, 2007). The stage of rapid spreading of the Tethys Ocean and its surrounding area occurred at the Middle to Late Jurassic transition (e.g., Matyja, 2009). The range of the spreading was determined mainly by palaeomagnetic data (Lewandowski et al., 2005, 2006). Matyja and Wierzbowski (2006) reported the relationship of these dynamic extensional processes around the Middle to Late Jurassic boundary in the outer basins of the Tethys Ocean. Extensional processes could have triggered heat flow increase in the crust (Allen and Allen, 2005). Moreover, strike-slip faults and associated structures were widely documented in the HCM. The strike-slip fault sets form a complex network, which developed during Late Paleozoic and Mesozoic time (Konon, 2007). The damage zones of exhumed strike-slip faults dissecting Jurassic carbonates in the SW part of the HCM area revealed second-order faults and fractures infilled with syntectonic calcite. The subsequent development of a structural pattern of microscopic fault-related structures and calcite infills shows the activity of faults (Rybak-Ostrowska et al., 2020). These permeable fault-related structures were likely important pathways of fluid flow. Microstructural, stable isotope and fluid inclusion data indicate that calcite precipitated primarily during strike-slip fault movement (Rybak-Ostrowska et al., 2020).

Additionally, in some borehole sections in the northern part of the margin of the HCM, the influence of fluid flow seems also to be an important factor. The Jurassic to Lower Carboniferous section in the Nieświń PIG 1 borehole displayed VR values ranging from 0.56 to 1.73% VR (Grotek, 2018). In this section at least two VR gradients can be identified instead of one, and the break between them occurs within a continuous sedimentary section of the Middle Triassic. Therefore, it excludes any exhumation related to unconformities, that might have indicated the influence of post-Triassic fluid flow heating. In the Opoczno PIG-2 borehole, VR data from the Jurassic to the Lower Carboniferous (Swadowska, 2006) shows a rapid VR increase from 0.48% in the Jurassic to up to 1.6% in the Lower Triassic, finally decreasing in Zechstein strata (to 1.3% VR) in an almost sub-vertical profile. Such a non-linear VR section also suggests post-Triassic fluid flow. In the same section, there is also a VR jump at the unconformity between Zechstein (1.37%) and Lower Carboniferous (2.44%) strata. Therefore, pre-Permian heat flow or/and burial caused significant thermal maturation of Carboniferous organic matter. Generally, mapping of VR data from the NE area of the HCM, including some boreholes of the Miechów Trough, shows thermal maturity in Triassic strata (0.8–1.2% VR) which is higher than in Zechstein strata: 0.5–1.0% VR (Grotek, 2018). This strongly implies that fluid flow occurred extensively after the Triassic.

Regional stratigraphic evidence, combined with thermal maturity data and supported by apatite fission-track data, and zircon helium data in adjacent areas (Botor et al., 2018; Łuszczak et al., 2020), leads to the suggestion that at least two phases of fluid flow events happened also in the Miechów Trough: the first one during late Carboniferous–early Permian time and another during Jurassic time. This results of this study match with the thermal maturity modeling results of Poprawa et al. (2005) who described thermal maturity depth profiles in the Mesozoic successions of the HCM that suggested a Late Jurassic phase of hot fluid migration, presumably related to enhanced permeability of faults and fractures driven by extension. Poprawa et al. (2005), though, inferred two discrete phases of fluid circulation: in the late Carboniferous to early Permian and then in the Late Jurassic, while their model emphasized that the late Jurassic event was mainly responsible for the Devonian-Carboniferous thermal maturity. However, in the borehole sections analysed, the VR pattern break at the base of the Permian unconformity is evidence against there being only one, late Mesozoic, thermal event. Moreover, zircon helium ages from Ordovician to early Carboniferous strata show that a distinct cooling event occurred during the transition from the late Carboniferous to early Permian (Botor et al., 2018). Furthermore, in the SW part of the HCM (Kowala and Ostrówka bentonites), the apatite fission track record indicates slow cooling throughout the Mesozoic and Cenozoic (Botor et al., 2018).

The study area of the Miechów Trough is situated along the KLFZ, which is likely part of the trans-European fault zone extending from Hamburg to the Black Sea area (Żaba, 1999). Tectono-thermal activity along the KLFZ could have played an important role in the development of the thermal maturity pattern in the study area, particularly in maturation of organic matter and petroleum generation within the pre-Permian deposits (e.g., Bełka and Siewniak-Madej, 1996). In the boreholes of the Miechów Trough analysed, the relatively low conodont CAI values of 1 in the Triassic rocks indicates that the Devonian and Lower Carboniferous strata must have reached their thermal maturity earlier, most likely in the late Carboniferous (Malec, 2015). The regionally distributed low thermal maturity data (below ~0.5% VR) in the Mesozoic deposits are also evidence against an increase in thermal maturity within Paleozoic strata after the Permian (Kołcoń and Wagner, 1983; Marynowski et al., 2007; Marynowski and Wyszomirski, 2008; Rybicki et al., 2016, 2017). Miocene deposits in the Carpathian Foredeep also show low (below 0.5% VR) thermal maturity (Szafran and Wagner, 1999, 2000; Więcław et al., 2011; Kotarba et al., 2017). Conodont CAI data from the Silurian strata on the SW margin of the Małopolska Block display a relatively uniform thermal overprint (CAI values of 4) caused by maximum burial in the early Pennsylvanian. The estimated maximum temperatures of ~200–220°C can be explained by elevated heat flow, with a paleogeothermal gradient of ~60–70°C/km, associated with extensional stage of development of the KLFZ. This thermal maturation level was locally enhanced (CAI values up to 8) in the latest Carboniferous to early Permian (~300 Ma, Mikulski et al., 2019), due to the magmatic and hydrothermal activity caused by Variscan regional extension (Bełka and Siewniak-Madej, 1996). Along the KLFZ there occur porphyry-type Mo-Cu-W ore deposits (e.g., Oszczepalski et al., 2010; Mikulski et al., 2019) of Variscan origin. A Variscan collision of continent–continent type between the Bohemian Massif and Brunovistulicum caused a reactivation of the Upper Silesian Block and the Małopolska Block margins, leading to widespread magmatism along the KLFZ (Mikulski et al., 2019). The magmatism involved bimodal calc-alkaline rocks (granitoids and dacitoides), accompanied by alkaline volcanic rocks of mafic-intermediate composition, e.g. lamprophyres and diabases (Słaby et al., 2010). Although the geodynamic model of structural evolution of the KLFZ is still a matter of debate, magma emplacement can be correlated with regional strike-slip tectonic activity (Mikulski et al., 2019).

Generally, multiple hydrothermal activities, mainly during the Jurassic, can be traced around the Palaeo-Atlantic all over western and central Europe, suggesting fluid circulation on a wide regional scale. With fluid temperatures in excess of

~150–200°C at shallow crustal levels, and considering pervasive heating of the basement due to continent-wide rifting events during the opening of the North-Atlantic, these hydrothermal events would have substantially altered the palaeothermal field (e.g., Timar-Geng et al., 2004).

## CONCLUSIONS

Integrated VR analysis and thermal maturity modeling were applied to establish the burial and thermal evolution of the Miechów Trough. This allowed the following conclusions:

(1) The thermal maturity of organic matter dispersed in the Lower Paleozoic to Cretaceous succession is in the range of 0.49 to 3.06% of mean random VR. This allowed estimation of maximum palaeotemperatures of the analysed rocks ranging from 78 to 225°C for a burial-induced model and from 71 to 295°C for a hydrothermal-induced model.

(2) The pre-Zechstein Variscan thermal regime was different to the Mesozoic one. At least two fluid flow events might be identified.

(3) The maximum palaeotemperature (~120–290°C) in the Silurian to lower Carboniferous sedimentary succession was achieved in the late Carboniferous to early Permian. The late Variscan tectonic activity may have been triggered by increased heat flow that was, at least partly, coupled with fluid circulation.

(4) The maximum palaeotemperature (~70–150°C) of the Zechstein to Jurassic sedimentary succession was achieved during the Middle to Late Jurassic. It was likely caused by a hot fluid flow event related to extensional tectonics.

(5) The hydrocarbon potential of the Paleozoic source rocks was depleted before the Upper Jurassic and Cenomanian reservoir rocks and traps were formed. Consequently, the majority of hydrocarbons generated during pre-Late Jurassic time were lost.

**Acknowledgements**. This work was supported by AGH project no 16.16.140.315. Particular thanks are given to late Prof. Marian Wagner (AGH, Kraków) for discussion of organic petrography aspects and vitrinite reflectance measurements, and to Dr. Chris Clayton (CCGS, Tenbury Wells, Worcestershire, UK) for very valuable discussion of organic geochemistry aspects. I would like to thank the reviewers: Prof. L. Marynowski, Dr. A. Feldman-Olszewska and Prof. P.H. Karnkowski, for taking the necessary time and effort to review the manuscript. I sincerely appreciate all the valuable comments and suggestions, which helped me improve the quality of the manuscript. Special thanks go to the editor for the significant coordination of the review and publication processes.

## REFERENCES

**Allen, P.A., Allen J.R., 2005.** Basin Analysis: Principles and Applications. Blackwell Publishing, Oxford, UK.

**Barker, C.E., 1983**. Influence of time on metamorphism of sedimentary organic matter in liquid-dominated geothermal systems, western North America. Geology, **11**: 384–388; https://doi.org/10.1130/0091-7613(1983)11%3C384:IOTOMO%3E2.0.CO;2

**Barker, C.E., Pawlewicz, M.J. 1994.** Calculation of vitrinite reflectance from thermal histories and peak temperatures. A comparison of methods. ACS Symposium series, **570**: 216–229.

**Bełka, Z., 1990.** Thermal maturation and burial history from conodont colour alteration data, Holy Cross Mountains, Poland. Courier Forschungsinstitut Senckenberg, **118**: 241–251.

**Bełka, Z., 1993.** Thermal and burial history of the Cracow-Silesia region (southern Poland) assessed by conodont CAI analysis. Tectonophysics, **227**: 161–190; https://doi.org/10.1016/0040-1951(93)90093-Y

**Bełka, Z., Siewniak-Madej, A., 1996**. Thermal maturation of the Lower Palaeozoic strata in the southwestern margin of the Małopolska Massif, southern Poland: no evidence for Caledonian regional metamorphism. Geologische Rundschau, **85**: 775–781.

**Bossennec, C., Géraud, Y., Böcker, J., Klug, B., Mattioni, L., Bertrand, L., Moretti, I., 2021.** Characterization of fluid flow conditions and paths in the Buntsandstein Gp. sandstones reservoirs, Upper Rhine Graben. Bulletin de la Société Géologique de France, **192**, 35; https://doi.org/10.1051/bsgf/2021027

**Botor, D., 2021**. Burial and thermal history modeling of the Paleozoic–Mesozoic basement in the northern margin of the Western Outer Carpathians (case study from Pilzno-40 well, southern Poland). Minerals, **11**, 733; https://doi.org/10.3390/min11070733

**Botor, D., 2023**. Hydrocarbon generation modeling in the Permian and Triassic strata of the Polish Basin: implications for hydrocarbon potential assessment. Geological Quarterly, **67,** 20; https://doi.org/10.7306/gq.1690

**Botor, D., Anczkiewicz, A.A., Dunkl, I., Golonka, J., Paszkowski, M., Mazur, S., 2018**. Tectonothermal history of the Holy Cross Mountains (Poland) in the light of low-temperature thermochronology. Terra Nova, **30**: 270–278; https://doi.org/10.1111/ter.12336

**Botor, D., Golonka, J., Zając, J., Papiernik, B., Guzy, P., 2019.** Petroleum generation and expulsion in the Lower Palaeozoic petroleum source rocks in the SW margin of the East European Craton (Poland). Annales Societatis Geologorum Poloniae, **89**: 153–174; https://doi.org/10.14241/asgp.2019.11

**Buła, Z., Jachowicz, M. Żaba, J., 1997**. Principal characteristics of the Upper Silesia Block and Małopolska Block border zone (southern Poland). Geological Magazine, **134**: 669–677; https://doi.org/10.1017/S0016756897007462

**Buła, Z., Habryn, R., Jachowicz-Zdanowska, M., Żaba, J., 2015**. The Pre-Cambrian and Lower Paleozoic of the Brunovistulicum (eastern part of the Upper Silesian Block, southern Poland) – the state of the art. Geological Quarterly, **59** (1): 123–134; https://doi.org/10.7306/gq.1203

**Cattò, S., 2014.** Tectonic evolution of the Holy Cross Mountains (Poland). Ph.D. Thesis, Padua University, Italy.

**Cavailhes, T., Rotevatn, A., Monstad, S., Khala, A.B., Funk, E., Canner, K., Looser, M., Chalabi, A., Gay, A., Travé, A., Ferhi, F., Skanji, A., Chebbi, R.M., Bang, N., 2018.** Basin tectonic history and paleo-physiography of the Pelagian platform, northern Tunisia, using vitrinite reflectance data. Basin Research, **30**: 926–941; https://doi.org/10.1111/bre.12287

**Connolly, C.A., 1989.** Thermal history and diagenesis of the Wilrich Member shale, Spirit River Formation, northwest Alberta. Canadian Petroleum Geology Bulletin, **37**: 182–197; https://doi.org/10.35767/gscpgbull.37.2.182

**Curtis, J.B., Kotarba, M.J., Lewan, M.D., Więcław, D., 2004.** Oil/source rock correlations in the Polish Flysch Carpathians and Mesozoic basement and organic facies of the Oligocene Menilite Shales: insights from hydrous pyrolysis experiments. Organic Geochemistry, **35**: 1573–1596; https://doi.org/10.1016/j.orggeochem.2004.06.018

**Dadlez, R., Marek, S., Pokorski, J., 2000**. Geological Map of Poland without Cainozoic Deposits, scale 1:1 000 000. Państwowy Instytut Geologiczny, Warszawa.

**Dadlez, R., Narkiewicz, M., Stephenson, R.A., Visser, M.T.M., Van Wees, J.D., 1995.** Tectonic evolution of the Mid-Polish Trough: modeling implications and significance for central European geology. Tectonophysics, **252**: 179–195; https://doi.org/10.1016/0040-1951(95)00104-2

**Derkowski A., Środoń, J., Goryl, M., Marynowski, L., Szczerba, M., Mazur, S., 2021.** Long-distance fluid migration defines the diagenetic history of unique Ediacaran sediments in the East European Craton**.** Basin Research, **33**: 570–593; https://doi.org/10.1111/bre.12485

**Dudek, L., Strzetelski, J., Botor, D., Florek, R., 2003.** Petroleum potential of the Mesozoic-Paleozoic basement in the Bochnia–Tarnów area (in Polish with English summary). Prace Instytutu Górnictwa Naftowego i Gazownictwa, **122**: 1–68.

**Fijałkowska-Mader, A., 2020.** Application of the TAI (Thermal Alteration Index) and palynofacial analysis for determining the degree of organic matter thermal maturity in the Upper Permian and Triassic deposits in the northern part of the Nida Basin (central Poland) (in Polish with English summary). Nafta-Gaz, (8): 495–500; https://doi.org/10.18668/NG.2020.08.01

**Filipiak, P., Jurczak-Drabek, A., Karwasiecka, M., Krieger, W., 2002**. Organic matter in the clastic and coal-bearing Carboniferous deposits of Jachówka-2K, Sułkowice-1, Wysoka-3 and Zawoja-1 boreholes (in Polish with English summary). Przegląd Geologiczny, **50**: 752–761.

**Florek, R., Górka, A., Zacharski, J., 2006**. Wpływ architektury mezo–paleozoicznego podłoża miocenu na warunki migracji i akumulacji węglowodorów w utworach cenomanu i części przedgórza Karpat (in Polish). Prace Instytutu Górnictwa Naftowego i Gazownictwa, **137**: 231–239.

**Frings, U., Lutz, R., de Wall, H., Warr, L.N., 2004.** Coalification history of the Cinera-Matallana pull-apart basin (NW Spain). International Journal of Earth Sciences, **93**: 92–106; https://doi.org/10.1007/s00531-003-0370-7

**Gliniak, P., Gutowski, J., Urbaniec, A., 2005**. Organic buildups recognized upon well and seismic data within the Upper Jurassic formations of the Carpathian foreland, Poland; perspectives for hydrocarbon exploration. Volumina Jurassica**,** **3**: 29–43.

**Górka, A., Gliniak, P., Madej, K., Maksym, A., 2007**. Oil and gas fields in the Carpathians and the Carpathian Foredeep (in Polish with English summary). Przegląd Geologiczny, **55**: 993–998.

**Grotek, I., 2000.** Charakterystyka petrograficzna materii organicznej (in Polish). In: Ropo- i gazonośność osadów permu i triasu w północnej części niecki nidziańskiej (eds. M. Kuleta, S. Zbroja, A. Iwanow and H. Kiersnowski). Narodowe Archiwum Geologiczne PIG–PIB, Kielce.

**Grotek, I., 2008**. Charakterystyka petrograficzna oraz dojrzałość termiczna materii organicznej (in Polish). In: Malec J. (red.). Potencjał węglowodorowy utworów paleozoiku i mezozoiku północno-zachodniego obrzeżenia Gór Świętokrzyskich. Narodowe Archiwum Geologiczne PIG–PIB, Kielce.

**Grotek, I., 2018**. Charakterystyka petrograficzna oraz dojrzałość termiczna materii organicznej rozproszonej w utworach karbonu-jury (in Polish). Profile Głębokich Otworów Wiertniczych Państwowego Instytutu Geologicznego, **151**: 141–146.

**Gutowski J., Koyi, H.A., 2007.** Influence of oblique basement strike-slip faults on the Mesozoic evolution of the south-eastern segment of the Mid-Polish Trough. Basin Research, **19**: 67–86; https://doi.org/10.1111/j.1365-2117.2007.00312.x

**Hackley, P.C., Araujo, C.V., Borrego, A.G., Bouzinos, A., Cardott, B.J., Cook, A.C., Eble, C., Flores, D., Gentzis, T., Goncalves, P.A., Mendonca Filho, J.G., Hamor-Vido, M., Jelonek, I., Kommeren, K., Knowles, W., Kus, J., Mastalerz, M., Menezes, T.R., Newman, J., Oikonomopoulos, J.K., Pawlewicz, M., Pickel, W., Potter, J., Ranasinghe, P., Read, H., Reyes, J., De La Rosa Rodriguez, G., de Souza, I.V.A.F., Suarez-Ruiz, I., Sykorova, I., Valentine, B.J., 2015.** Standardization of reflectance measurements in dispersed organic matter: Results of an exercise to improve interlaboratory agreement. Marine and Petroleum Geology, **59**: 22–34; https://doi.org/10.1016/j.coal.2018.06.004

**Hantschel, T., Kauerauf, A., 2009.** Fundamentals of Basin and Petroleum Systems Modeling. Springer, Heidelberg.

**Hartkopf-Fröder, C., Königshof, P., Littke, R., Schwarzbauer, J., 2015**. Optical thermal maturity parameters and organic geochemical alteration at low grade diagenesis to anchimetamorphism: a review. International Journal of Coal Geology, **150–151**: 74–119; https://doi.org/10.1016/j.coal.2015.06.005

**Incerpi, N., Martire, L., Manatschal, G., Bernasconi, S.M., Gerdes, A., Czuppon, G., Palcsu, L., Karner, G.D., Johnson, C.A., Figueredo, P.H., 2020**. Hydrothermal fluid flow associated to the extensional evolution of the Adriatic rifted margin: Insights from the pre- to post-rift sedimentary sequence (SE Switzerland, N Italy). Basin Research, **32**: 1–25; https://doi.org/10.1111/bre.12370

**Joachimski, M.M., Ostertag-Henning, C., Pancost, R.D., Strauss, H., Freeman, K.H., Littke, R., Damste, J.S.S., Racki, G., 2001**. Water column anoxia, enhanced productivity and concomitant changes in $^{13}C$ and $^{34}S$ across the Frasnian–Famennian boundary (Kowala, Holy Cross Mountains/Poland). Chemical Geology, **175**: 109–131; https://doi.org/10.1016/S0009-2541(00)00365-X

**Jurkiewicz, H., 1975**. The geological structure of the basement of the Mesozoic in the central part of the Miechów Trough (in Polish with English summary). Biuletyn Instytutu Geologicznego, **283**: 1–100.

**Jurkiewicz, H. (ed.), 1974**. Milianów IG 1 (in Polish). Profile Głębokich Otworów Wiertniczych Instytutu Geologicznego, **21**: 1–104.

**Jurkiewicz, H. (ed.), 1976a**. Pągów IG 1 (in Polish). Profile Głębokich Otworów Wiertniczych Instytutu Geologicznego, **33**: 1–85.

**Jurkiewicz, H. (ed.), 1976b**. Jaronowice IG 1 (in Polish). Profile Głębokich Otworów Wiertniczych Instytutu Geologicznego, **34**: 1–117.

**Jurkiewicz, H. (ed.), 1980**. Potok Mały IG 1 (in Polish). Profile Głębokich Otworów Wiertniczych Instytutu Geologicznego, **51**: 1–88.

**Jurkiewicz, H. (ed.), 1990**. Włoszczowa IG 1 (in Polish). Profile Głębokich Otworów Wiertniczych Państwowego Instytutu Geologicznego, **70**: 1–56.

**Jurkowska, A., 2016.** Inoceramid stratigraphy and depositional architecture of the Campanian and Maastrichtian of the Miechów Synclinorium (southern Poland), Acta Geologica Polonica, **66**: 59–84; https://doi:10.1515/agp-2015-0025

**Kalinowski, A.A., Gurba, L.W., 2020.** Interpretation of vitrinite reflectance–depth profiles in the Northern Denison Trough, Bowen Basin, Australia. International Journal of Coal Geology, **219**, 1033667; https://doi.org/10.1016/j.coal.2019.103367

**Karnkowski, P.H., 2007.** Petroleum Provinces in Poland. Przegląd Geologiczny, **55**: 1061–1067.

**Kołcoń, I., Wagner, M., 1983.** Brown coal within ore-bearing dolomites of the Zn-Pb deposit in the "Pomorzany" mining area near Olkusz (in Polish with English summary). Kwartalnik Geologiczny, **27** (4): 739–754.

**Konon, A., 2006**. Buckle folding in the Kielce Unit, Holy Cross Mountains, central Poland. Acta Geologica Polonica, **56**: 375–405.

**Konon, A., 2007.** Strike-slip faulting in the Kielce Unit, Holy Cross Mountains, central Poland. Acta Geologica Polonica, **57**: 415–441.

**Kosakowski, P., Więcław, D., Kotarba, M.J., Kowalski, A., 2012**. Habitat and hydrocarbon potential of the Mesozoic strata in the Kraków–Rzeszów area (SE Poland). Geological Quarterly, **56** (1): 139–152.

**Kotarba, M.J., Więcław, D., Bilkiewicz, E., Dziadzio, P., Kowalski, A., 2017**. Genetic correlation of source rocks and natural gas in the Polish Outer Carpathians and Paleozoic–Mesozoic basement east of Kraków (southern Poland). Geological Quarterly, **61** (4): 795–824; https://doi.org/10.7306/gq.1367

**Kowalska, S., Wójtowicz, A., Hałas, S., Wemmer, K., Mikołajewski, Z., Buniak, A., 2019.** Thermal history of Lower Palaeozoic rocks from the East European Platform margin of Poland based on K-Ar age dating and illite-smectite palaeothermometry. Annales Societatis Geologorum Poloniae, **89**: 481–509; https://doi.org/10.14241/asgp.2019.21

**Kozłowska, A., Poprawa, P., 2004.** Diagenesis of the Carboniferous clastic sediments of the Mazowsze region and the northern Lublin region related to their burial and thermal history (in Polish with English summary). Przegląd Geologiczny, **52**: 491–500.

**Krzywiec, P., 2002**. Mid-Polish Trough inversion – seismic examples, main mechanisms and its relationship to the Alpine-Carpathian collision, European Geosciences Union, Stephan Mueller Special Publication Series, **1**: 151–165.

**Krzywiec, P., Gągała, Ł., Mazur, S., Słonka, Ł., Kufrasa, M., Malinowski, M., Pietsch, K., Golonka, J., 2017a.** Variscan deformation along the Teisseyre-Tornquist Zone in SE Poland: Thick-skinned structural inheritance or thin-skinned thrusting? Tectonophysics, **718**: 83–91; https://doi.org/10.1016/j.tecto.2017.06.008

**Krzywiec, P., Mazur, S., Gągała, Ł., Kufrasa, M., Lewandowski, M., Malinowski, M., Buffenmyer, V., 2017b**. Late Carboniferous thin-skinned compressional deformation above the SW edge of the East European craton as revealed by seismic reflection and potential field data – Correlations with the Variscides and the Appalachians. GSA Memoir, **213**: 353–372; https://doi.org/10.1130/2017.2013(14)

**Krzywiec, P., Stachowska, A., Stypa, A., 2018.** The only way is up – on Mesozoic uplifts and basin inversion events in SE Poland. Geological Society Special Publications, **469**: 33–57; https://doi.org/10.1144/sp469.14

**Kuberska, M., Kiersnowski, H., Poprawa, P., Kozłowska, A., 2021.** Rotliegend sedimentary rocks in the Kutno-2 well under conditions of a postulated Jurassic thermal event and high overpressure – a petrographic study (in Polish with English abstract). Przegląd Geologiczny, **69**: 365–373; https://doi.org/10.7306/2021.19

**Kuberska, M., Kozłowska, A., Wołkowicz, K., 2023**. Triassic and Jurassic siliciclastic rocks of the Łódź-Miechów Syncline in the aspect of the development of their pore space (in Polish with English summary). Przegląd Geologiczny, **71**: 212–218; https://doi.org/10.7306/2023.16

**Lamarche, J., Mansy, J., Bergerat, F., Averbuch, O., Hakenberg, M., Lewandowski, M., Stupnicka, E., Świdrowska, J., Wajsprych, B., Wieczorek, J., 1999.** Variscan tectonics in the Holy Cross Mountains (Poland) and the role of structural inheritance during Alpine tectonics. Tectonophysics, **313**: 171–186; https://doi.org/10.1016/S0040-1951(99)00195-X

**Lamarche, J., Lewandowski, M., Mansy, J.L., Szulczewski, M., 2003a**. Partitioning pre-, syn-and post-Variscan deformation in the Holy Cross Mountains, eastern Variscan foreland. Geological Society Special Publications, **208**: 159–184; https://doi.org/10.1144/gsl.sp.2003.208.01.08

**Lamarche, J., Scheck, M., Lewerenz, B., 2003b**. Heterogeneous tectonic inversion of the Mid-Polish Trough related to crustal architecture, sedimentary patterns and structural inheritance. Tectonophysics, **373**: 75–92; https://doi.org/10.1016/S0040-1951(03)00285-3

**Lampe, C., Person, M., Nöth, S., Ricken, W., 2001.** Episodic fluid flow within continental rift basins: some insights from field data and mathematical models of the Rhinegraben. Geofluids, **1**: 42–52; https://doi.org/10.1046/j.1468-8123.2001.11005.x

**Laughland, M., Underwood, M.B., 1993.** Vitrinite reflectance and estimates of paleotemperature within the Upper Shimanto Group, Muroto Peninsula, Shikoku, Japan. GSA Special Paper, **273**: 25–43; https://doi.org/10.1130/SPE273-p45

**Lewan, M.D., Kotarba, M.J., Curtis, J.B., Więcław, D., Kosakowski, P., 2006**. Oil generation kinetics for organic facies with Type-II and -IIS kerogen in the Menilite Shales of the Polish Carpathians. Geochimica and Cosmochimica Acta, **70**: 3351–3368; https://doi.org/10.1016/j.gca.2006.04.024

**Lewandowski, M., Krobicki, M., Matyja, B.A. Wierzbowski, A. 2005.** Palaeogeographic evolution of the Pieniny Klippen Basin using stratigraphic and palaeomagnetic data from the Veliky Kamenets section (Carpathians, Ukraine). Palaeogeography, Palaeoclimatology, Palaeoecology, **216**: 53–72; https://doi.org/10.1016/j.palaeo.2004.10.002

**Lewandowski, M., Aubrecht, R., Krobicki, M., Matyja, B.A., Rehakova, D., Schlogl, J., Sidorczuk, M., Wierzbowski, A., 2006.** Palaeomagnetism of the Pieniny Klippen Belt (Carpathians): evidence for low-latitude origin and palaeogeographic dispersion of the Upper Jurassic carbonates. Volumina Jurassica, **4**: 56–58.

**Łuszczak, K., Wyglądała, M., Śmigielski, M., Waliczek, M., Matyja, B.A., Konon, A., Ludwiniak, M., 2020**. How to deal with missing overburden - investigating Late Cretaceous exhumation of the Mid-Polish anticlinorium by a multi-proxy approach. Marine and Petroleum Geology, **114**, 104229; https://doi.org/10.1016/j.marpetgeo.2020.104229

**Majorowicz, J., Polkowski, M., Grad, M., 2019**. Thermal properties of the crust and the lithosphere–asthenosphere boundary in the area of Poland from the heat flow variability and seismic data. International Journal of Earth Sciences, **108**: 649–672; https://doi.org/10.1007/s00531-018-01673-8

**Malec, J., 2015**. Thermal maturity of Devonian, Carboniferous and Triassic rocks in the central part of the Małopolska Massif from conodont Colour Alteration Index (in Polish with English summary). Biuletyn Państwowego Instytutu Geologicznego, **462**: 29–39.

**Malec, J., Więcław, D., Zbroja, S., 2010.** The preliminary assessment of the selected Paleozoic formations of the Holy Cross Mountains. Geologia Kwartalnik AGH, **36**: 5–24.

**Marynowski, L., Wyszomirski, P., 2008**. Organic geochemical evidence of early-diagenetic oxidation of the terrestrial organic matter during the Triassic arid and semi-arid climatic conditions. Applied Geochemistry, **23**: 2612–2618; https://doi.org/10.1016/j.apgeochem.2008.05.011

**Marynowski, L., Czechowski, F., Simoneit, B.R.T., 2001.** Phenylnaphthalenes and polyphenyls in Palaeozoic source rocks of the Holy Cross Mountains, Poland. Organic Geochemistry, **32**: 69–85; https://doi 10.1016/S0146-6380(00)00150-9

**Marynowski, L., Salamon, M., Narkiewicz, M., 2002**. Thermal maturity and depositional environments of organic matter in the post-Variscan succession of the Holy Cross Mountains. Geological Quarterly, **46** (1): 25–36.

**Marynowski, L., Zatoń, M., Simoneit, B.R.T., Otto, A., Jędrysek, M.O., Grelowski, C., Kurkiewicz S., 2007**. Compositions, sources and depositional environments of organic matter from the Middle Jurassic clays of Poland. Applied Geochemistry, **22**: 2456–2485; https://doi.org/10.1016%2Fj.apgeochem.2007.06.015

**Marynowski, L., Filipiak, P., Zatoń, M., 2010**. Geochemical and palynological study of the Upper Famennian Dasberg event horizon from the Holy Cross Mountains (central Poland). Geological Magazine, **147**: 527–550.

**Matyasik, I., Dziadzio, P., 2006.** Reconstruction of petroleum systems based on integrated geochemical and geological investigations: Selected examples from the middle Outer Carpathians in Poland. AAPG Memoir, **84**: 497–518; https://doi.org/10.1306/M84985

**Matyja, B., 2009**. Development of the Mid-Polish Trough versus Late Jurassic evolution in the Carpathian Foredeep area. Geological Quarterly, **53** (1): 49–62.

**Matyja, B.A., Wierzbowski, A., 2006**. Field trip B2 — Open shelf facies of the Polish Jura Chain. In: Jurassic of Poland and Adjacent Slovakian Carpathians (eds. A. Wierzbowski et al.): 198–204. Field trip guidebook. 7th International Congress on the Jurassic System, 6–18 September 2006, Kraków, Poland.

**Mazur, S., Mikołajczak, M., Krzywiec, P., Malinowski, M., Buffenmyer, V., Lewandowski, M., 2015**. Is the Teisseyre-Tornquist Zone an ancient plate boundary of Baltica? Tectonics, **34**: 2465–2477; https://doi.org/10.1002/2015TC003934

**Mazur, S., Aleksandrowski, P., Gągała, Ł., Krzywiec, P., Żaba, J.,·Gaidzik, K., Sikora, R., 2020**. Late Palaeozoic strike-slip tectonics versus oroclinal bending at the SW outskirts of Baltica:

case of the Variscan belt's eastern end in Poland. International Journal of Earth Sciences, **109**: 1133–1160; https://link.springer.com/article/10.1007/s00531-019-01814-7

**Migaszewski, Z.M., Hałas, S., 1996**. The age and origin of the calcite mineralization in the Holy Cross Mts based on lithologic-petrographic and isotopic evidence. Przegląd Geologiczny, **44**: 275–282.

**Migaszewski, Z.M., 2002**. K-Ar and Ar-Ar dating of diabases and lamprophyres from the Holy Cross Mts. (in Polish with English summary). Przegląd Geologiczny, **50**: 227–229.

**Mikulski, S.Z., Williams, I.S.,·Markowiak, M., 2019**. Carboniferous-Permian magmatism and Mo-Cu (W) mineralization in the contact zone between the Małopolska and Upper Silesia Blocks (south Poland): an echo of the Baltica-Gondwana collision. International Journal of Earth Sciences, **108**: 1467–1492; https://doi.org/10.1007/s00531-019-01715-9

**Moryc, W., 2006a**. Geological structure of Miocene substratum in Kraków-Pilzno region. Part 1. The Pre- Cambrian and Paleozoic (without Permian) (in Polish with English summary). Nafta-Gaz, (5**)**: 197–216.

**Moryc, W., 2006b**. Geological structure of Miocene substratum in Kraków-Pilzno region. Part 2. The Permian and Mesozoic period (in Polish with English summary). Nafta-Gaz, (6**)**: 263–282.

**Moryc, W., 2014**. The Permian and Triassic of the Polish Carpathian Foreland (in Polish with English summary). Biuletyn Państwowego Instytutu Geologicznego, **457**: 43–68.

**Naglik, B., Toboła, T., Natkaniec-Nowak, L., Luptáková, J., Milovská, S., 2016.** Raman spectroscopic and microthermometric studies of authigenic quartz (the Pepper Mts., Central Poland) as an indicator of fluids circulation. Spectrochimica Acta Part A Molecular and Biomolecular Spectroscopy, **173:** 960–964; https://doi.org/10.1016/j.saa.2016.10.047

**Narkiewicz, M., 2002**. Ordovician through earliest Devonian development of the Holy Cross Mts. (Poland): constraints from subsidence analysis and thermal maturity data. Geological Quarterly, **46** (3): 255–266.

**Narkiewicz, M., 2007**. Development and inversion of Devonian and Carboniferous basins in the eastern part of the Variscan foreland (Poland). Geological Quarterly, **51** (3): 231–256.

**Narkiewicz, M., 2017.** Comment on a paper by Schito et al. (2017) "Thermal evolution of Paleozoic successions of the Holy Cross Mountains (Poland)". Marine and Petroleum Geology, **88**: 1109–1113; https://doi.org/10.1016/j.marpetgeo.2017.02.016

**Narkiewicz, M., 2020.** The Variscan foreland in Poland revisited: new data and new concepts. Geological Quarterly, **64** (2): 377–401; https://doi.org/10.7306/gq.1511

**Narkiewicz, M., Resak, M., Littke, R., Marynowski, L., 2010.** New constraints on the Middle Palaeozoic to Cenozoic burial and thermal history of the Holy Cross Mts. (central Poland): results of numerical modeling. Geologica Acta, **8**: 189–205; https://doi.org/10.1344/105.000001529

**Nawrocki, J., Salwa, S., Pańczyk, M., 2013**. New $^{40}$Ar-$^{39}$Ar age constrains for magmatic and hydrothermal activity in the Holy Cross Mts. (southern Poland). Geological Quarterly, **57** (3): 551–560; https://doi.org/10.7306/gq.1117

**Nemčok, M., Henk, A., 2006**. Oil in foreland sourced by thrustbelt: insights from numerical stress modeling and balancing in the West Carpathians. Geological Society Special Publications, **253**: 415–428; https://doi.org/10.1144/GSL.SP.2006.253.01.22

**Oszczepalski, S., Markowiak, M., Mikulski, S.Z., Lasoń, K, Buła, Z., Habryn, R., 2010.** Porphyry Mo–Cu–W mineralization within Precambrian-Paleozoic rocks – prospectivity analysis of the border zone of the Upper Silesia and Małopolska Blocks (in Polish with English summary). Biuletyn Państwowego Instytutu Geologicznego, **439**: 339–354.

**Oszczypko, N., Krzywiec, P., Popadyuk, I., Peryt, T., 2006**. Carpathian Foredeep Basin (Poland and Ukraine): Its sedimentary, structural, and geodynamic evolution. AAPG Memoir, **84**: 293–350; https://doi.org/10.1306/985612M843072

**Papiernik, B., Łapinkiewicz, A.P., Górecki, W., 2007**. Petrophysical conditions of oil and gas productivity of Devonian and Carboniferous deposits in the southern part of the Miechów Trough in the light of computer modeling results (in Polish with English abstract). Geologia Kwartalnik AGH, **33**: 341–374.

**Papiernik, B., Botor, D., Golonka, J., Porębski, S.J., 2019**. Unconventional hydrocarbon prospects in Ordovician and Silurian mudrocks of the East European Craton (Poland): Insight from three-dimensional modeling of total organic carbon and thermal maturity. Annales Societatis Geologorum Poloniae, **89**: 511–533; https://doi.org/10.14241/asgp.2019.26

**Pharaoh, T.C., 1999**. Paleozoic terranes and their lithospheric boundaries within the Trans-European Suture Zone (TESZ): a review. Tectonophysics, **314**: 17–41; https://doi.org/10.1016/S0040-1951(99)00235-8

**Pletsch, T., Appel, J., Botor, D., Clayton, C. J., Duin, E. J. T., Faber, E., Górecki, W., Kombrink, H., Kosakowski, P., Kuper, G., Kus, J., Lutz, R., Mathiesen, A., Ostertag, C., Papiernik, B., Van Bergen, F., 2010.** Petroleum generation and migration. In: Petroleum Geological Atlas of the Southern Permian, Basin Area (eds. J.C. Doornenbal and A.G. Stevenson): 225–253. EAGE Publications, Houten, Holland.

**Poprawa, P., Żywiecki, M., Grotek, I., 2005.** Burial and thermal history of the Holy Cross Mts. area-preliminary results of maturity modeling. Polskie Towarzystwo Mineralogiczne, Prace Specjalne, **26:** 251–254.

**Pożaryski, W., Karnkowski, P., 1992.** Mapa tektoniczna Polski w epoce waryscyjskiej 1: 1 000 000 (in Polish). Wyd. Geol., Warszawa.

**Rakociński, M., Marynowski, L., Zatoń, M., Filipiak, P., 2021.** The mid-Tournaisian (Early Carboniferous) anoxic event in the Laurussian shelf basin (Poland): an integrative approach. Palaeogeography, Palaeoclimatology, Palaeoecology, **566**, 110236; https://doi.org/10.1016/j.palaeo.2021.110236

**Resak, M., Narkiewicz, M., Littke, R., 2008**. New basin modeling results from the Polish part of the Central European Basin system: implications for the Late Cretaceous–Early Paleogene structural inversion. International Journal of Earth Sciences, **97**: 955–972; https://doi.org/10.1007/s00531-007-0246-3

**Rybak-Ostrowska B., Konon, A., Hurai, V., Bojanowski, M., Konon, A., Wyglądała, M., 2020**. Fluid pathways within shallow-generated damage zones of strike-slip faults – evidence of map-scale faulting in a continental environment, SW Permo-Mesozoic cover of the Late Palaeozoic Holy Cross Mountains Fold Belt, Poland. Acta Geologica Polonica, **70**: 1–29; https://doi.org/10.24425/agp.2019.126454

**Rybicki, M., Marynowski, L., Misz-Kennan, M., Simoneit, B.R.T., 2016**. Molecular tracers preserved in Lower Jurassic ''Blanowice brown coals" from southern Poland at the onset of coalification: Organic geochemical and petrological characteristics. Organic Geochemistry, **102**: 77–92; https://doi.org/10.1016/j.orggeochem.2016.09.012

**Rybicki, M., Marynowski, L., Stukins, S., Nejbert, K., 2017.** Age and origin of the well-preserved organic matter in internal sediments from the Silesian-Cracow lead-zinc deposits, southern Poland. Economic Geology, **112**: 775–798; https://doi.org/10.2113/econgeo.112.4.775

**Scheck-Wenderoth, M., Krzywiec, P., Zülke, R., Maystrenko, Y., Frizheim, N., 2008.** Permian to Cretaceous tectonics. In: The Geology of Central Europe, **2**: Mesozoic and Cenozoic (ed. T. McCann): 999–1030. Geological Society, London, United Kingdom.

**Schito, A., Corrado, S., Trolese, M., Aldega, L., Caricchi, C., Cirilli, S., Grigo, D., Guedes, A., Romano, C., Spina, A., Valentim, B., 2017**. Assessment of thermal evolution of Paleozoic successions of the Holy Cross Mountains (Poland). Marine and Petroleum Geology, **80:** 112–132; https://doi.org/10.1016/j.marpetgeo.2016.11.016

**Smolarek, J., Marynowski, L., Spunda, K., Trela, W., 2014**. Vitrinite equivalent reflectance of Silurian black shales from the Holy Cross Mountains, Poland. Mineralogia, **45**: 79–96.

**Smolarek, J., Trela, W., Bond, DPG, Marynowski L., 2017a**. Lower Wenlock black shales in the northern Holy Cross Mountains, Poland: sedimentary and geochemical controls on the Ireviken Event in a deep marine setting. Geological Magazine, **154**: 247–264; https://doi.org/10.1017/S0016756815001065

**Smolarek, J., Marynowski, L., Trela, W., Kujawski, P., Simoneit BRT., 2017b**. Redox conditions and marine microbial community changes during the end-Ordovician mass extinction event. Global and Planetary Change, **149**: 105–122; https://doi.org/10.1016/j.gloplacha.2017.01.002

**Słaby, E., Breitkreuz, C., Żaba, J., Domańska-Siuda, J., Gajdzik, K., Falenty, K., Falenty, A., 2010**. Magma generation in an alternating transtensional–transpressional regime, the Kraków-Lubliniec Fault Zone, Poland. Lithos, **119**: 251–268; https://doi.org/10.1016/j.lithos.2010.07.003

**Słonka, Ł., Krzywiec, P., 2020**. Upper Jurassic carbonate buildups in the Miechów Trough, southern Poland – insights from seismic data interpretations. Solid Earth, **11**: 1097–1119; https://doi.org/10.5194/se-11-1097-2020

**Suchý, V., Filip, J., Sýkorová, I., Pešek, J., Kořínková, D., 2019**. Palaeo-thermal and coalification history of Permo-Carboniferous sedimentary basins of Central and Western Bohemia, Czech Republic: first insights from apatite fission track analysis and vitrinite reflectance modeling. Bulletin of Geosciences, **94**: 201–219; https://doi.org/10.3140/bull.geosci.1696

**Swadowska, E., 2006**. Petrograficzna charakterystyka rozproszonej materii organicznej (in Polish). Profile Głębokich Otworów Wiertniczych Państwowego Instytutu Geologicznego. **111**: 73–75.

**Sweeney, J.J., Burnham, A.K., 1990**. Evaluation of a simple model of vitrinite reflectance based on chemical kinetics. AAPG Bulletin, **74**: 1559–1570; https://doi.org/10.1306/0C9B251F-1710-11D7-8645000102C1865D

**Szafran, S., Wagner, M., 1999**. Petrologic studies of Miocene organic matter in the Carpathian Foredeep, southern Poland (in Polish with English summary). Zeszyty Naukowe Politechniki Śląskiej – Seria Górnictwo, **243**: 131–138.

**Szafran, S., Wagner, M., 2000**. Geotectonic causes of changes in mean reflectance of huminit/vitrinite coalified organic material in Miocene sediments of Carpathian Foredeep (in Polish with English summary). Zeszyty Naukowe Politechniki Śląskiej – Seria Górnictwo, **246**: 517–532.

**Szaniawski, R., 2008**. Late Paleozoic geodynamics of the Małopolska Massif in the light of new paleomagnetic data for the southern Holy Cross Mountains. Acta Geologica Polonica, **58**: 1–12.

**Szulczewski, M., 1995.** Depositional evolution of the Holy Cross Mts. (Poland) in the Devonian and Carboniferous-a review. Geological Quarterly, **39** (4): 471–488.

**Środoń, J., Trela, W., 2012**. Preliminary clay mineral data on burial history of the Holy Cross Mts., Poland. Mineralogia – Special Papers, **39**: 93–94.

**Taylor, G. H., Teichmuller, M., Davis, A., Diessel, C. F. K., Littke, R., Robert, P., 1998.** Organic Petrology: A New Handbook Incorporating Some Revised Parts of Stach's Textbook of Coal Petrology. Gebruder Borntraeger, Berlin.

**Ten Haven, H.L., Lafargue, E., Kotarba, M., 1993**. Oil/oil and oil/source rock correlations in the Carpathian Foredeep and Overthrust, southeast Poland. Organic Geochemistry, **20**: 935–959; https://doi.org/10.1016/0146-6380(93)90105-K

**Timar-Geng, Z., Fügenschuh, B., Schaltegger, U., Wetzel, A., 2004.** The impact of the Jurassic hydrothermal activity on zircon fission track data from the southern Upper Rhine Graben area. Schweizerische Mineralogische und Petrographische Mitteilungen, **84**: 257–269.

**Tobin, R.C., Claxton, B.L., 2000.** Multidisciplinary thermal maturity studies using vitrinite reflectance and fluid inclusion microthermometry: a new calibration of old techniques. AAPG Bulletin, **84**: 1647–1665; https://doi.org/10.1007/BF00435311

**Tóth, J., 2009.** Gravitational Systems of Groundwater Flow: Theory, Evaluation, Utilization. Cambridge University Press, Cambridge, UK.

**Verweij, H.M., Souto Carneiro Echternach, M., Witmans, N., Abdul Fattah, R., 2012**. Reconstruction of basal heat flow, surface temperature, source rock maturity, and hydrocarbon generation in salt dominated Dutch Basins. AAPG Hedberg Series, **4**: 175–195; https://doi.org/10. 1306/13311 435H4 3470

**Waliczek, M., Machowski, G., Więcław, D., Konon, A., Wandycz, P., 2019**. Properties of solid bitumen and other organic matter from Oligocene shales of the Fore-Magura Unit in Polish Outer Carpathians: Microscopic and geochemical approach. International Journal of Coal Geology, **210**, 103206; https://doi.org/10.1016/j.coal.2019.05.013

**Waliczek, M., Machowski, G., Poprawa, P., Świerczewska, A., Więcław, D., 2021.** A novel $VR_o$, Tmax, and S indices conversion formulae on data from the fold-and-thrust belt of the Western Outer Carpathians (Poland). International Journal of Coal Geology, **234**, 103672; https://doi.org/10.1016/j.coal.2019.05.013

**Waples, D.W., 1980**. Time and temperature in petroleum formation: application of Lopatin's method to petroleum exploration. AAPG Bulletin **64**: 916–926; https://doi.org/10.1306/03B5A665-16D1-11D7-8645000102C1865D

**Waples, D., Kamata, H., Suizu M., 1992a.** The art of maturity modeling, part 1: finding of a satisfactory model. AAPG Bulletin, **76**: 31–46; https://doi.org/10.1306/BDFF875E-1718-11D7-8645000102C1865D

**Waples, D., Kamata, H., Suizu, M., 1992b**. The art of maturity modeling, part 2: alternative models and sensitivity analysis. AAPG Bulletin, **76**: 47–66; https://doi.org/10.1306/BDFF8768-1718-11D7-8645000102C1865D

**Więcław, D., 2011.** Origin of liquid hydrocarbons accumulated in the Miocene strata of the Polish Carpathian Foredeep and its Paleozoic-Mesozoic basement. Annales Societatis Geologorum Poloniae, **81**: 443–458.

**Więcław, D., Kotarba, M.J., Kowalski, A., Kosakowski, P., 2011**. Habitat and hydrocarbon potential of the Palaeozoic source rocks in the Kraków-Rzeszów area (SE Poland). Annales Societatis Geologorum Poloniae, **81**: 375–394.

**Więcław, D., Kosakowski, P., Kotarba, M.J., Koltun, Y.V., Kowalski, A., 2012**. Assessment of hydrocarbon potential of the Lower Palaeozoic strata in the Tarnogród-Stryi area (SE Poland and western Ukraine). Annales Societatis Geologorum Poloniae, **82**: 65–80.

**Wójcik, K., Zacharski, J., Łojek, M., Wróblewska, S., Kiersnowski, H., Waśkiewicz, K., Wójcicki, A., Laskowicz, R., Sobień, K., Peryt, T., Chylińska-Macios, A., Sienkiewicz, J., 2022**. New opportunities for oil and gas exploration in Poland – a review. Energies, **15,** 1739; https://doi.org/10.3390/en15051739

**Wróbel, M., Kosakowski, P., Więcław, D., 2016**. Petroleum processes in the Paleozoic-Mesozoic strata of the Grobla-Limanowa area (basement of the Polish Carpathians). Geology, Geophysics and Environment, **42**: 185–206.

**Wygrala B., 1989.** Integrated Study of an Oil Field in the Southern Po Basin, Northern Italy. Ph.D. Thesis, University of Cologne, Cologne, Germany.

**Yamaji, A., 1986**. Analysis of vitrinite reflectance-burial depth relations in dynamical geological settings by direct integration method. Journal of Japan Association of Petroleum Technology, **51**: 1–8.

**Ziagos, J.P., Blackwell, D.D., 1986.** A model for the transient temperature effects of horizontal fluid flow in geothermal systems. Journal of Volcanology and Geothermal Research, **27**: 371–397; https://doi.org/10.1016/0377-0273(86)90021-1

**Ziegler, P.A., 1986**. Geodynamic model for the Palaeozoic crustal consolidation of Western and Central Europe. Tectonophysics, **126**: 303–328; https://doi.org/10.1016/0040-1951(86)90236-2

**Zielinski, G.W., Poprawa, P., Szewczyk, J., Grotek, I., Kiersnowski, H., Zielinski, R.L.B., 2012**. Thermal effects of Zechstein salt and the Early to Middle Jurassic hydrothermal event in the central Polish Basin. AAPG Bulletin, **96**: 1981–1996; https://doi.org/10.1306/04021211142

**Zielińska, M., 2017.** Organic-matter vitrinite reflectance variability in the Outer Carpathians, Poland: Relationship to tectonic evolution. Geological Quarterly, **61** (1): 214–226; https://doi.org/10.7306/gq.1338

**Zielińska, M., Jirman, P., Gedl, P., Botor, D., 2023.** Burial and thermal history of the eastern transform boundary of the central western Carpathians based on 1D basin modeling. Marine and Petroleum Geology, **147**, 106021; https://doi.org/10.1016/j.marpetgeo.2022.106021

**Zwing, A., 2003**. Causes and mechanisms of remagnetisation in Palaeozoic sedimentary rocks - a multidisciplinary approach. Ph.D. Thesis. Fakultät für Geowissenschaften der Ludwig-Maximilians-Universität München, Germany.

**Żaba, J., 1999**. The structural evolution of Lower Paleozoic succession in the Upper Silesia Block and Małopolska Block border zone, southern Poland (in Polish with English summary). Prace Państwowego Instytutu Geologicznego, **166**: 1–162.

**Żelaźniewicz, A., Pańczyk, M., Nawrocki, J., Fanning, M., 2008.** A Carboniferous/Permian, calc-alkaline, I-type granodiorite from the Małopolska Block, Southern Poland: implications from geochemical and U-Pb zircon age data. Geological Quarterly, **52** (4): 301–308.

**Żelaźniewicz, A., Aleksandrowski, P., Buła, Z., Karnkowski, P., Konon, A., Oszczypko, N., Ślączka, A., Żaba, J., Żytko, K., 2011.** Tectonic subdivision of Poland (in Polish). Komitet Nauk Geologicznych PAN, Wrocław, Poland.

**Żelaźniewicz, A., Oberc-Dziedzic, T., Fanning, C.M., Protas, A., Muszyński, A., 2016**. Late Carboniferous-Early Permian events in the Trans-European Suture Zone: tectonic and acid magmatic evidence from Poland. Tectonophysics, **675**: 227–243; https://doi.org/10.1016/j.tecto.2016.02.040